(19) Europäisches Patentamt
European Patent Office
Office européen des brevets

(11) **EP 3 770 302 A1**

(12) **EUROPEAN PATENT APPLICATION**

(43) Date of publication:
27.01.2021 Bulletin 2021/04

(51) Int Cl.:
C25B 1/00 *(2021.01)* ***C25B 1/10*** *(2006.01)*
C25B 9/08 *(2006.01)* ***C25B 11/04*** *(2021.01)*

(21) Application number: **19305971.4**

(22) Date of filing: **22.07.2019**

(84) Designated Contracting States:
AL AT BE BG CH CY CZ DE DK EE ES FI FR GB GR HR HU IE IS IT LI LT LU LV MC MK MT NL NO PL PT RO RS SE SI SK SM TR
Designated Extension States:
BA ME
Designated Validation States:
KH MA MD TN

(71) Applicants:
- **L'AIR LIQUIDE, SOCIETE ANONYME POUR L'ETUDE ET L'EXPLOITATION DES PROCEDES GEORGES CLAUDE**
  75007 Paris (FR)
- **Université Paris Diderot Paris 7**
  75013 Paris (FR)
- **CENTRE NATIONAL DE LA RECHERCHE SCIENTIFIQUE - CNRS**
  75016 Paris 16 (FR)

(72) Inventors:
- **BRAUN, Waldemar**
  65929 Frankfurt am Main (DE)
- **JOULIE, Dorian**
  92170 Vanves (FR)
- **BOUDY, Benjamin**
  75018 Paris (FR)
- **TORBENSEN, Kristian**
  75010 Paris (FR)
- **ROBERT, Marc**
  75019 Paris (FR)

(74) Representative: **A.P.I. Conseil**
Immeuble Newton
4, rue Jules Ferry
64000 Pau (FR)

(54) **IRON AND COBALT MOLECULAR COMPLEXES FOR THE SELECTIVE ELECTROCHEMICAL REDUCTION OF CO2 INTO CO, WITH FLOW CELLS**

(57) The present invention concerns a flow cell electrolyzer (1) to electrochemically reduce reagent gas CO_2 into gaseous CO and gaseous H2, with an anodic compartment comprising an anode (2) with a current collector, and on the current collector, at least a catalyst to electrochemically oxidize H2O to O_2, an anodic electrolyte solution (3) at a controlled flow rate Q_a, comprising: a solvent, and an anodic electrolyte, the solvent being water at neutral or basic pH ; a cathodic compartment comprising a cathodic electrolyte solution (6), at a controlled flow rate Q_c, comprising: the solvent, and a cathodic electrolyte, the solvent being water at neutral or basic pH, a gas diffusion porous cathode (9) which comprises, on a gas diffusion porous current cathode collector which is electrochemically inert, at least a molecular catalyst on a surface S to electrochemically reduce CO_2 into CO, with a by-production of H_2, the molecular catalyst being chosen between the list with the metal chosen among: Iron, Cobalt: metal porphyrin with one or several $^{+}N(C_1\text{-}C_4$ alkyl$)_3$ groups, metal phthalocyanine, metal phthalocyanine with one or several $^{+}N(C_1\text{-}C_4$ alkyl$)_3$ groups, or cobalt quater pyridine.

Figure 14

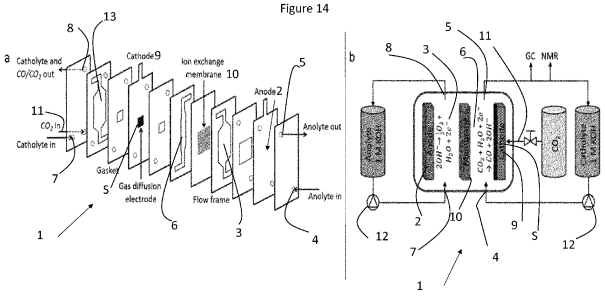

EP 3 770 302 A1

Description

FIELD OF THE INVENTION

[0001] The present invention relates to iron and cobalt molecular complexes as catalysts for the highly selective electrochemical reduction of CO_2 into CO, with electrochemical cells comprising them.

STATE OF ART

[0002] Despite the increasingly frequent use of renewable energies to produce electricity and avoid concomitant production of CO_2, it is reasonable to consider that CO_2 emissions, in particular resulting from energy production, will remain high in the next decades. Thus, it appears necessary to find ways to capture CO_2 gas, either for storing or valorization purposes.

[0003] Indeed, CO_2 can also be seen, not as a waste, but on the contrary as a source of carbon. For example the promising production of synthetic fuels from CO_2 and water has been envisaged.

[0004] However, CO_2 exhibits low chemical reactivity: breaking its bonds requires an energy of 724 kJ/mol. Moreover, CO_2 electrochemical reduction to one electron occurs at a very negative potential, thus necessitating a high energy input, and leads to the formation of a highly energetic radical anion ($CO_2^{\cdot-}$). Catalysis thus appears mandatory in order to reduce CO_2 and drive the process to multi-electronic and multi-proton reduction process, in order to obtain thermodynamically stable molecules. In addition, direct electrochemical reduction of CO_2 at inert electrodes is poorly selective, yielding formic acid in water, while it yields a mixture of oxalate, formate and carbon monoxide in low-acidity solvents such as DMF.

[0005] CO_2 electrochemical reduction thus requires catalytic activation in order to reduce the energy cost of processing, and increase the selectivity of the species formed in the reaction process.

[0006] Molecular catalysts that combine high selectivity and high current density for CO_2 electrochemical reduction to CO or other chemical feedstocks, are in high demand. Molecular transition metal catalysts offer the distinct advantage of allowing for the fine-tuning of the primary and secondary coordination spheres by manipulating the chelating environment and the steric and electronic effects of the ligands. The ability to improve catalytic efficiency and product selectivity through the rational optimization of the ligand structure is a feature not accessible to the solid-state catalysts common to pilot-scale electrolyser units.[1-2] There now exists a range of known molecular catalysts, including those based on noble (e.g. Ru, Ir and Re) and earth-abundant metals (e.g. Co, Ni, Fe, Mn and Cu). [1-9] These catalysts typically trigger a two electron reduction of CO_2 to either CO or formate with reasonable efficiencies, but in organic solvents.

[0007] The integration of above described molecules by applying thin porous carbon films, such as carbon powder, carbon nanotubes or graphene to form hybrid catalytic materials, has proven to be a promising strategy to selectively achieve CO production in pure aqueous conditions. Reasonable performances have been obtained in nearly neutral conditions (pH 7-7.5) with good selectivity.[10,11] While these performances represent advances for CO2RR (CO_2 reduction reaction) catalysts, much higher current densities are required for commercial operation, being highly selective and operating at low overpotentials at the same time. Moreover, these current densities remain far below those obtained with state-of-the-art solid-state Ag[12,13] or Au[14] nanomaterials have been reported to reach >150 mA/cm^2.

SUMMARY OF THE INVENTION

[0008] Here, the invention presents a flow cell electrolyzer to electrochemically reduce reagent gas CO_2 into gaseous CO and gaseous H_2, with:

- an anodic compartment comprising:
  - an anode with a current collector, and on the current collector, at least a catalyst to electrochemically oxidize H_2O to O_2,
  - an anodic electrolyte solution, at a controlled flow rate Q_a, comprising: a solvent, and an anodic electrolyte, the solvent being water,

  the anodic compartment being connected to an anodic electrolyte solution inlet and an anodic electrolyte solution outlet;

- a cathodic compartment comprising:
  - a cathodic electrolyte solution, at a controlled flow rate Q_c, comprising: a solvent, and a cathodic electrolyte,

the solvent being water, the cathodic compartment being connected to a cathodic electrolyte solution inlet and a cathodic electrolyte solution outlet,

- a gas diffusion porous cathode which comprises, on a gas diffusion porous current cathode collector which is electrochemically inert, at least a molecular catalyst incorporated in the porous cathode with a surface S, to electrochemically reduce CO_2 into CO, with a by-production of H_2,

the molecular catalyst being chosen between the list:

- ❖ metal porphyrin with one or several $+N(C_1\text{-}C_4\ alkyl)_3$ groups, with the metal chosen among: Iron, Cobalt;
- ❖ metal phthalocyanine, with the metal chosen among: Iron, Cobalt;
- ❖ metal phthalocyanine with the metal chosen among: Iron, Cobalt, with one or several groups among: $+N(C_1\text{-}C_4\ alkyl)_3$, F, $C(CH_3)$, or
- ❖ cobalt quater pyridine

- an anion exchange membrane, impermeable to CO_2, CO, H_2 and O_2, between the anodic compartment and the cathodic compartment;

- a channel for flowing the reagent gas CO_2, at a controlled flow rate Q_g, onto or through the surface S of the gas diffusion porous current cathode collector;

- all flow rates are controlled by passing the cathodic and anodic electrolytes as well as the reagent gas through pump means serving to:

  - ◦ circulate by pumping the anodic electrolyte solution and the cathodic electrolyte solution between the inlet and the outlet,
  - ◦ flow by pumping the reagent gas CO_2 onto or through the gas diffusion porous cathode;

- a power supply providing the energy necessary to trigger the electrochemical reactions involving the reagent.

BRIEF DESCRIPTION OF THE DRAWINGS

[0009] Other advantages and characteristics of the disclosed devices and methods will become apparent from reading the description, illustrated by the following figures, where:

Figure 1. Current density and CO selectivity recorded at various potentials. Recorded in CO_2 saturated 0.5 M $NaHCO_3$ (pH 7.3). Each potential step was maintained for 20 min.

Figure 2. Current density and CO selectivity recorded during a 24 hour electrolysis at -0.78 V vs RHE in CO_2 saturated 0.5 M $NaHCO_3$. The cell potential was 3.41 V.

Figure 3. Applied potential and CO selectivity recorded under chronopotentiometric conditions at 50 $mAcm^{-2}$ for 3 hours in CO_2 saturated 0.5 M $NaHCO_3$. The cell potential was 4.05 V.

Figure 4. Applied potential and CO selectivity recorded under chronopotentiometric conditions at 50 $mAcm^{-2}$ for 3 hours in CO_2 saturated 1.0 M $NaHCO_3$. The cell potential was 3.46 V.

Figure 5. (A) Current density and CO selectivity at various cell temperatures. Recorded in CO_2 saturated 0.5 M $NaHCO_3$. (B) Arrhenius plot constructed from the TOF values calculated for each temperature step in (A).

Figure 6. Current density and CO selectivity recorded at various potentials. Recorded in 1.0 M KOH solution (pH 14). Each potential step was maintained for 20 min.

Figure 7. Applied potential and CO selectivity recorded under chronopotentiometric conditions at 27 $mAcm^{-2}$ for 24 hours in 1.0 M KOH. The cell potential was 1.87 V.

Figure 8. Applied potential and CO selectivity recorded under chronopotentiometric conditions at 50 $mAcm^{-2}$ for 3 hours in 1.0 M KOH. The cell potential was 2.36 V.

Figure 9. Step potential experiment, giving the current density recorded at various potentials. Recorded in CO_2 saturated 0.5 M $NaHCO_3$ (pH 7.3). Each potential step was maintained for 20 min.

Figure 10. Step potential experiment, giving the current density recorded at various potentials. Recorded in argon saturated 0.5 M $NaHCO_3$ (pH 7.3) at a film formulated with the non-metalated porphyrin ligand. Each potential step was maintained for 20 min.

Figure 11. Current density and CO selectivity recorded during a 6 hour electrolysis at -0.78 V vs RHE in CO_2 saturated 1 M $NaHCO_3$.

Figure 12. Step potential experiment, giving the current density recorded at various potentials. Recorded in 1 M KOH (pH 14). Each potential step was maintained for 20 min.

Figure 13. Step potential experiment, giving the current density recorded at various potentials. Recorded in 1 M KOH (pH 7.3) at a film formulated with the non-metalated porphyrin ligand. Each potential step was maintained for 20 min.

Figure 14. Cross-sectional view (a) and general scheme (b) of the CO_2 electrolyzer flow cell.

Figure 15. a: Current density for CO production as a function of the potential. b: Bulk electrolysis at fixed potential (E = - 0.72 V vs. RHE) for **CoPc2@**carbon black deposited onto a carbon paper as cathodic material, in 1 M KOH. c: Co K-edge XANES profiles of CoPc2 (black dots), and **CoPc2@**carbon black before and after electrolysis (E = - 0.72 V vs. RHE) which are superposed, in 1 M KOH solution.

Figure 16. Flow cell electrolyzer set-up.

Figure 17. Repetitive cyclic voltammetry for **CoPc1@**MWCNTs (bottom) and **CoPc2@**MWCNTs (top) films deposited onto a glassy carbon electrode (d = 3 mm) in 0.5 M $NaHCO_3$ solution saturated with CO_2 (pH 7.3; black, 1st scan; grey, 2nd scan), at v = 0.1 V s^{-1}.

Figure 18. SEM image of a catalytic film deposited onto carbon paper.

Figure 19. Blank experiments: Left, at E = -0.676 V vs. RHE) in the absence of catalyst in CO_2 saturated 0.5 M $NaHCO_3$ solution (pH =7.3); right, at E = -0.605 V vs. RHE with **CoPc2@**MWCNTs (1:15) in Ar saturated 0.5 M $NaHCO_3$ solution (pH =8.5). In both cases, only H_2 was detected as reaction product.

Figure 20. Variation of the total current density as a function of the electrolysis potential at optimized mass ratio for **CoPc1@**MWCNTs in a CO_2 saturated solution containing 0.5 M $NaHCO_3$ (pH 7.3).

Figure 21. Co 2p (left) and N 1s (right) XPS spectra before and after a 7h electrolysis (E = -0.676 V vs. RHE) with **CoPc2@**MWCNTs with a 1:15 ratio in a CO_2 saturated solution with 0.5 M $NaHCO_3$ (pH 7.3).

Figure 22. Bulk electrolysis at E= -0.971 V vs. RHE of a CO_2 saturated solution containing 0.5 M KCl (pH 4) using **CoPc2@**MWCNTs as catalyst.

Figure 23. Total current density as a function of the applied potential for **CoPc2@**carbon black deposited onto a carbon paper as cathodic catalytic material, in 1 M KOH solution (flow cell device, see main text). Each potential step was held for a duration of 20 min.

Figure 24. Top: K-space (insert) and Fourier transform EXAFS spectra of **CoPc2@**carbon black before (black) and after electrolysis (E= -0.72 V vs RHE) (grey) in 1 M KOH solution.
Bottom: Co K-edge XANES spectra of the **CoPc2@**carbon black electrode after electrolysis (E = -0.72 V vs RHE) (red) together with those of reference compounds CoO (purple), CoOOH (orange), Co_3O_4 (blue) and metallic Co (green).

Figure 25. Bulk electrolysis at fixed current density (75 mA cm^{-2}) with **CoPc2@**carbon black deposited onto a carbon paper as cathodic catalytic material, in 1 M KOH solution (flow cell device, see main text). During the electrolysis, 2.5 g KOH were added every half hour into the cathode solution to maintain the pH balance.

Figure 26. CO Selectivity as a function of time in hours at 50 mA/cm^2 with **Co(qpy)** catalyst in a zero gap cell device.

DETAILED DESCRIPTION

[0010] The present invention concerns: a flow cell electrolyzer 1 to electrochemically reduce a gas reactant comprising CO_2, into gaseous CO and gaseous H_2, with:

- an anodic compartment comprising:
  - an anode 2 with a current collector, and on the current collector, at least a catalyst to electrochemically oxidize H_2O to O_2,
  - an anodic electrolyte solution 3, at a controlled flow rate Q_a, comprising: a solvent, and an anodic electrolyte, the solvent being water, the anodic compartment being connected to an anodic electrolyte solution inlet 4 and an anodic electrolyte solution 3 outlet;
- a cathodic compartment comprising:
  - a cathodic electrolyte solution 6, at a controlled flow rate Q_c, comprising: a solvent, and a cathodic electrolyte, the solvent being water, the cathodic compartment being connected to a cathodic electrolyte solution inlet 7 and a cathodic electrolyte solution outlet 8,
  - a gas diffusion porous cathode 9 which comprises, on a gas diffusion porous current cathode collector which is electrochemically inert, at least a molecular catalyst incorporated in the porous cathode with a surface S, to electrochemically reduce CO_2 into CO, with a by-production of H_2.

[0011] The cathodic electrolyte can comprise a phosphate buffer or potassium hydroxide, and the anodic electrolyte comprises a phosphate buffer or potassium hydroxide.

[0012] The molecular catalyst is chosen between the list:

- ❖ metal porphyrin with one or several $+N(C_1\text{-}C_4\ alkyl)_3$ groups, with the metal chosen among: Iron, Cobalt
- ❖ metal phthalocyanine, with the metal chosen among: Iron, Cobalt
- ❖ metal phthalocyanine with the metal chosen among: Iron, Cobalt, with one or several groups among : $+N(C_1\text{-}C_4\ alkyl)_3$, F, $C(CH_3)_3$, or
- ❖ cobalt quater pyridine

[0013] The flow cell electrolyzer 1 comprises also:

- an anion exchange membrane 10, impermeable to CO_2, CO, H_2 and O_2, between the anodic compartment and the cathodic compartment;
- a channel 11 for flowing the reagent gas CO_2, at a controlled flow rate Q_g, onto or through the surface S of the gas diffusion porous current cathode collector;
- a power supply providing the energy necessary to trigger the electrochemical reactions involving the reagent.

[0014] In the flow cell electrolyzer 1, all flow rates are controlled by passing the cathodic and anodic electrolytes as well as the reagent gas through pump means 12 serving to:

- ◦ circulate by pumping the anodic electrolyte solution 3 and the cathodic electrolyte solution 6 between the inlets 4, and the outlets, 5,
- ◦ flow by pumping the reagent gas CO_2 onto or through the gas diffusion porous cathode 9;

[0015] In an example, the gas reactant comprises at least 99 % per volume CO_2, or at least 99,5 % per volume CO_2, or at least 99,9 % per volume CO_2, or at least 99,99 % per volume CO_2.

[0016] The flow cell 1 can have a device capable of recording the current generated by the electrochemical processes.

[0017] Advantageously, but in a non-limiting way, the channel for flowing the reagent gas CO_2 can comprise a flow frame generating a turbulent flow.

[0018] Advantageously, but in a non-limiting way, pumping means 12 to recirculate the anodic electrolyte solution 3 and the cathodic electrolyte solution 6.

[0019] In a preferred embodiment, the anodic and/or cathodic electrolyte solution has a neutral or basic pH.

[0020] In yet another preferred embodiment, the cathodic electrolyte solution has a basic pH. In such an embodiment, the anodic electrolyte solution may have an acidic or neutral pH.

[0021] In particular, the anodic electrolyte solution and/or the cathodic electrolyte solution has a pH from 9 to 14, preferably from 10 to 14, more preferably from 11.5 to 14, and more preferably from 13 to 14.

[0022] In yet another preferred embodiment, the cathodic electrolyte solution has a pH from 9 to 14, preferably from 10 to 14, more preferably from 11.5 to 14, and more preferably from 13 to 14. In such an embodiment, the anodic electrolyte solution may have an acidic or neutral pH.

[0023] Basic, i.e. alkaline conditions, in particular when applied to the cathodic electrolyte solution, allow operating the flow cell electrolyzer at surprisingly high current densities in comparison to acidic conditions.

[0024] The combination of basic conditions with the aforementioned molecular porphyrin, phthalocyanine or quater pyridine catalysts further result in surprisingly high selectivities for the desired conversion of CO_2 to CO, with only minor or even no side product formation. Thus, with the high current densities and high CO selectivity, the invention allows production of close-to-pure CO from CO_2 at high throughput rates.

[0025] Furthermore, it was found that the aforementioned molecular catalysts demonstrate high long-term stability even at harsh alkaline pH conditions.

[0026] The electrochemical reduction of the reagent into CO and H_2 can be carried out at ambient temperature.

[0027] The electrochemical reduction of the reagent into CO and H_2 can be carried out at atmospheric pressure.

[0028] Advantageously, the cathodic current collector can be carbon paper. On the carbon paper, a composite multilayered porous current collector (for instance a polytetrafluoroethylene gas distribution layer) can be filed to increase the reduction rate/efficiency.

[0029] In a realization, the porous cathode 9 comprises on the current collector an electrode film which, at least, contains polymers and the molecular catalysts. The electrode film can be filed in or grafted on the current collector.

[0030] Advantageously, when the molecular catalyst is a metal porphyrin, the metal porphyrin is a tetraphenylporphyrin which comprises specific groups on the phenyl moieties, with at least one or several $+N(C_1\text{-}C_4\ alkyl)_3$ groups among specific groups.

[0031] In a first embodiment of the flow cell electrolyzer 1, the molecular catalyst is the iron porphyrin with the formula:

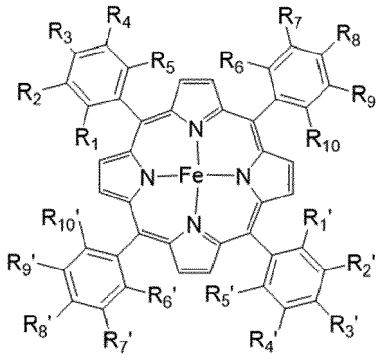

(I)

[0032] Wherein:

- at least 1 and at most 8 groups among R_1 to R_{10} and $R_{1'}$ to $R_{10'}$ being independently $+N(C_1\text{-}C_4\ alkyl)_3$ group,
- the remaining groups R_1 to R_{10} and $R_{1'}$ to $R_{10'}$ are independently selected from the group consisting of H, OH, F, $C(CH_3)_3$

[0033] In particular, the iron molecular catalyst can comprise:

- the other groups among R_1 to R_{10} and $R_{1'}$ to $R_{10'}$ are H; or
- the other groups among R_1 to R_{10} and $R_{1'}$ to $R_{10'}$ are H and F;

The iron molecular catalyst can comprise the $+N(C_1\text{-}C_4\ alkyl)_3$ groups in para or ortho position.

[0034] For instance: the molecular catalyst is an iron porphyrin FeTNT of formula (II):

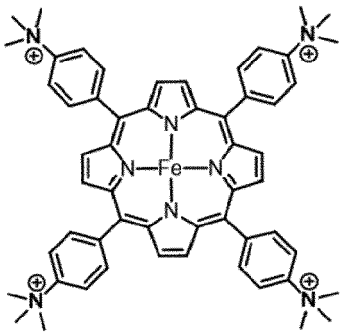

(II)

Or chosen among these iron containing molecules:

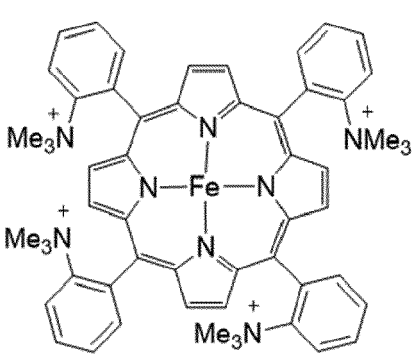

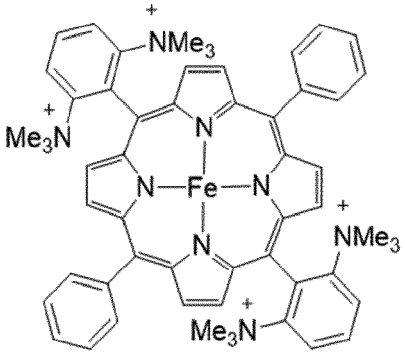

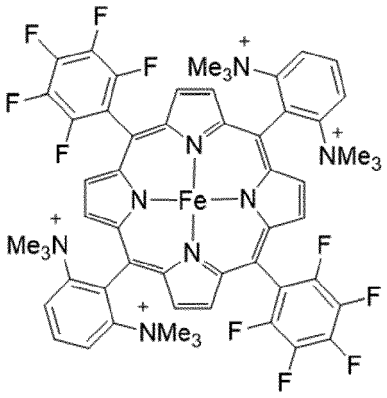

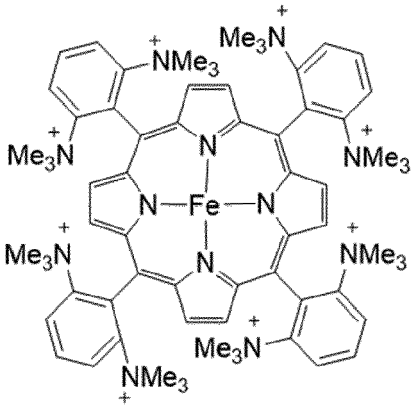

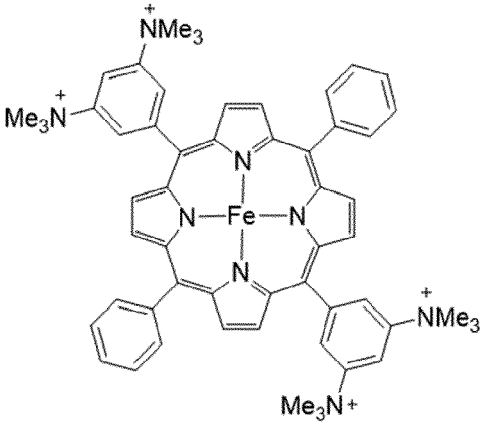

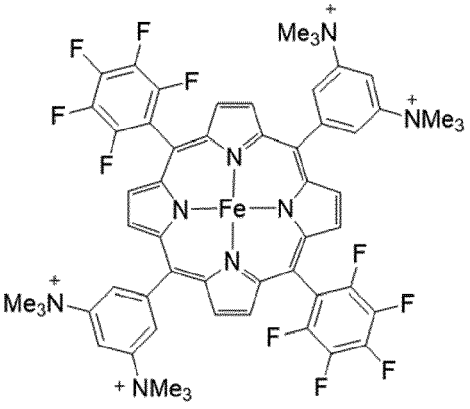

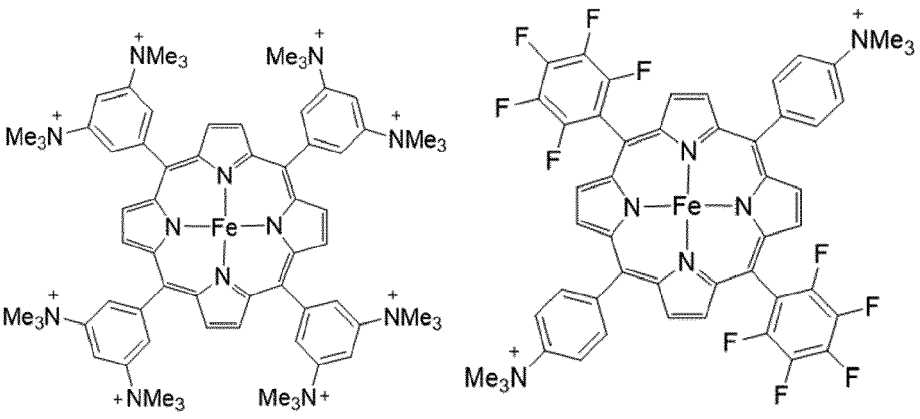

,preferably as its chloride salt.

[0035] With the iron porphyrin as molecular catalyst, at the operational conditions: the pH is between 7.3 and 14, and the potential applied to the cathode 9 is between 0 V and -1 V versus RHE (Reversible Hydrogen Electrode), the results of the flow cell can be: a current density for CO production of more than 5 and at least 150 $mA.cm^{-2}$, and the selectivity of the electrochemical reaction which is between 98% and 99.9%.

[0036] In a second embodiment of the flow cell electrolyzer 1, the flow cell electrolyzer 1 comprises the molecular catalyst which presents the formula:

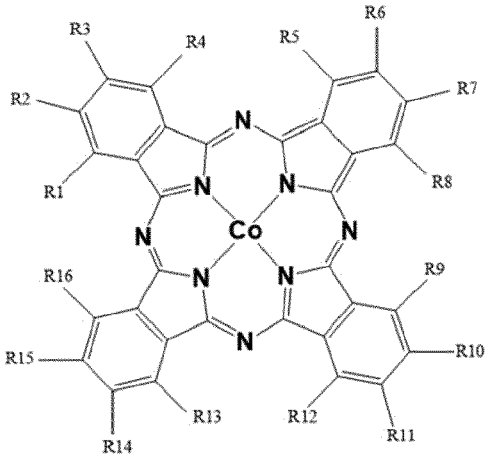

wherein R_1 to R_{16} are independently selected from the groups consisting of H, F, $C(CH_3)_3$ or $+N(C_1\text{-}C_4$ alkyl$)_3$

[0037] In particular, R_1 to R_{16} are H, and the molecular catalyst is a cobalt phthalocyanine CoPc of formula:

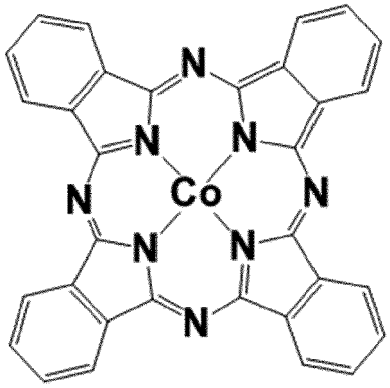

[0038] With the phthalocyanine as molecular catalyst, at the operational conditions: the pH is between 7.3 and 14, the potential applied to the cathode 9 is between -0.48 V and -0.98 V versus RHE, the results of the flow cell can be: a

current density for CO production of more than 10 and at least 50 $mAcm^{-2}$, and a selectivity of the electrochemical reaction between 90% and 92%.

[0039] In another variant, the cobalt molecular catalyst presents at least 1 and at most 8 groups among R_1 to R_{16} being independently $+N(C_1\text{-}C_4\ alkyl)_3$ group.

[0040] In another variant, the cobalt molecular catalyst presents for one or several of the specific following R_1, R_4, R_5, R_8, R_9, R_{12}, R_{13} and R_{16} groups, a $+N(C_1\text{-}C_4\ alkyl)_3$substituent.

[0041] For instance the molecular catalyst can be a cobalt phthalocyanine CoPc2 of formula:

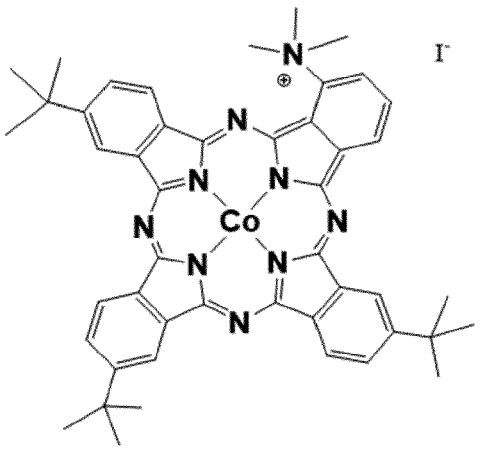

(III)

or the molecular catalyst is a cobalt phthalocyanine CoPc3 of formula:

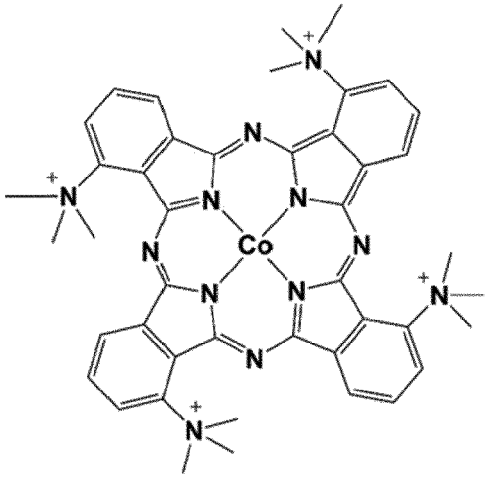

With the cobalt phthalocyanine with one or several $+N(C_1\text{-}C_4\ alkyl)_3$ groups, as molecular catalyst, at the operational conditions: the pH is between 7.3 and 14, and the potential applied to the cathode 9 is between -0.3 V and -1 V versus RHE, the results of the flow cell can be: a current density for CO production of more than 10 and at least 150 $mAcm^{-2}$, and a selectivity of the electrochemical reaction is between 92 % and 96 %.

[0042] In a third embodiment of the flow cell electrolyzer 1, the flow cell electrolyzer 1 comprises the molecular catalyst which presents the formulae of the cobalt quater pyridine

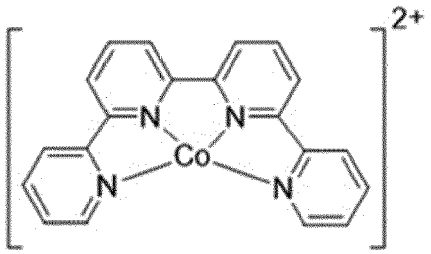

With the cobalt quater pyridine as molecular catalyst, at the operational conditions: the pH is between 7.3 and 14, and the potential applied to the cathode 9 is between -0.6 V and -1 V versus RHE, the results of the flow cell can be: a current density for CO production is between 25 and 200 $mAcm^{-2}$, and the selectivity of the electrochemical reaction is between 86.1 % and 98.8 %.

FIRST EMBODIMENT

Preparation of the hybrid materials for the gas diffusion electrode with **FeTNT**

[0043] 7.2 mg carbon black was dispersed in 8 mL ethanol by sonication for 30 min. A solution of 2.08 mg **FeTNT** in 2 mL ethanol was added to the carbon black suspension followed by sonication for 30 min. 20 μL of a 5% w/w Nafion solution was added followed by sonication for 30 min. The as prepared ink was disposed at 65°C on carbon paper masked with a PTFE frame to obtain a 1x1 cm^2 gas diffusion current collector.

Results

[0044] The inventors included **FeTNT** into a flow cell setup comprising **FeTNT** supported on a gas diffusion electrode as the cathode 9. Details of the setup are provided in the Supporting Information (see also Figures 14 and 16). Briefly, the electrolyzer consists of a sandwich of flow frames, electrodes, gaskets and an ion exchange membrane 10, which were assembled as schematically illustrated in Figure 14a. A gas flow of CO_2 is delivered from the back side of the cathodic compartment and flows through the gas diffusion electrode (GDE), while the catholyte solution is circulated in between the GDE and the anion exchange membrane 10 (AEM). On the other side of the AEM, the anolyte is directed between the AEM and the Pt/Ti alloy anode 2, Figure 14b. **FeTNT** was dispersed in a colloidal ink with carbon black and subsequently deposited on the carbon fiber paper, composing the cathode 9.

[0045] A survey of the catalytic activity as a function of applied potential was first performed in CO_2 saturated 0.5 M $NaHCO_3$. Figure 1 illustrates the increase in current density recorded for the CO_2RR as the overpotential was gradually set to more negative values by steps of 100 mV, along with the selectivity for CO production (see also Figure 9). Initially, at the less negative potentials, CO was detected as the only product; whereas minor amounts of H_2 stemming from the HER (Hydrogen Evolution Reaction) was observed at more negative potentials. The small amounts of the latter, even at potentials well beyond the HER onset, reflects the ability of the catalyst to strongly suppress the HER in favour of CO production. This was further verified by employing a non-catalytic film in the electrolyzer, i.e., a film formulated with the non-metalated porphyrin ligand, resulting in H_2 production exclusively (see Figure 10). The average current density and the CO selectivity at each applied potential is collected in Table 1 hereafter.

Table 1. Current densities and CO selectivity obtained with a catalytic film with FeTNTas catalyst (pH 7.3) as a function of the potential applied at the cathode 9.

E/V vs RHE	j_{av}/$mAcm^{-2}$	% CO
-0.38	7.2	99.9
-0.48	9.8	99.9
-0.58	14.8	99.8
-0.68	20.7	99.5
-0.78	27.2	99.3
-0.88	34.9	98.9
-0.98	42.1	98.6

[0046] The endurance of the catalytic film was tested by performing a chronoamperometric electrolysis for 24 hours. Based on the values listed in Table 1, a potential of -0.78 V vs RHE was chosen as this potential compromises between high current density and the ability of the catalyst to provide a nearly perfect CO production. The current density and the CO selectivity that have been obtained are shown in Figure 2, demonstrating the excellent stability of the system: a current density of 27.3 $mAcm^{-2}$ was maintained through the experiment with an average selectivity for CO of 98.2 ± 0.2%.

[0047] Under the same conditions, the cell performance was further evaluated by performing a chronopotentiometric electrolysis at a current density of 50 $mAcm^{-2}$. As shown in Figure 3, the cell maintained this current value for 3 hours at a potential of -1.14 V vs RHE. The product selectivity was not affected by the almost 2-fold current density increase, as CO was produced with a 98.3 ± 0.3% average selectivity.

[0048] In order to diminish the cell potential, the ohmic resistance of the cell was reduced by increasing the electrolyte concentration. This was demonstrated in a 1.0 M $NaHCO_3$ electrolyte solution, where a gain of >8 $mAcm^{-2}$ was obtained at an applied potential of -0.78 V vs RHE, without compromising the CO selectivity (see Figure 11). In a chronopotentiometric electrolysis, see Figure 4, the applied potential at 50 $mAcm^{-2}$ shifted positively to -0.86 V vs RHE, and in addition the cell potential was reduced by 590 mV. The CO product selectivity was 99.0 ± 0.2% on average.

[0049] A complementary approach to boost the cell performance was achieved by thermally activating the catalyst. During a chronoamperometric electrolysis at -0.78 V vs RHE, the catholyte temperature was incrementally increased from 24 °C to 34 °C and finally to 40 ºC. As shown in Figure 5A, an increase in current density was observed upon increasing the temperature, while maintaining the high CO product selectivity. Taking the TOF (in s^{-1}) as an apparent 1st order rate constant for the CO_2 conversion (assuming steady state conditions for the catalyst and proton source), an Arrhenius plot: ln(TOF) vs 1/T (in K^{-1}) was constructed (Figure 5B). From the slope, the activation energy, Ea, was calculated to 12 $kJmol^{-1}$.

[0050] In alkaline conditions (1.0 M KOH, pH 14) the cell performance was drastically improved. Figure 6 shows the resulting current densities and CO product selectivity recorded at various potentials (see also Figure 12). A current density of 6 $mAcm^{-2}$ was observed at 0.014 V vs RHE, and 155 $mAcm^{-2}$ was reached at -0.59 V vs RHE, with an excellent CO product selectivity, as summarized in Table 2. In a control experiment with the non-metalated porphyrin ligand, H_2 was the only detected product (see Figure 13).

Table 2. Current densities and CO selectivity obtained with a catalytic film with FeTNTas catalyst (pH 14) as a function of the potential applied at the cathode 9.

E/V vs RHE	j_{av}/$mAcm^{-2}$	% CO
0.014	6.0	99.9
-0.086	16.5	99.9
-0.19	37.6	99.9
-0.29	62.9	99.8
-0.39	89.7	99.5
-0.49	122.4	99.2
-0.59	155.2	98.1

[0051] To investigate the endurance of the catalyst in alkaline conditions, a chronopotentiometric electrolysis was performed at 27 $mAcm^{-2}$ for 24h, the same current density value as performed in pH-neutral conditions. As shown in Figure 7, a potential of ca. -0.16 V vs RHE was measured over the 24 hour course, showing only a minute increase. The CO product selectivity remained extremely high: 99.7 ± 0.2% on average.

[0052] For a direct comparison with the pH-neutral 1.0 M bicarbonate system, a chronopotentiometric electrolysis was performed at 50 $mAcm^{-2}$ in 1.0 M KOH, as shown in Figure 8. Over the course a 3 hours electrolysis, the applied potential remained stable (-0.23 V vs RHE), a very weakly negative potential for such high current density. Again, the CO selectivity was nearly perfect, with an average value of 99.8 ± 0.1%.

SECOND EMBODIMENT

[0053] The inventors included **CoPc2** into the same flow cell setup described in the first embodiment. **CoPc2** was supported on a gas diffusion electrode as the cathode 9. Details of the setup are provided in the Supporting Information (see Figure 16). **CoPc2** was dispersed in a colloidal ink with carbon black and subsequently deposited on the carbon fiber paper, composing the cathode 9.

[0054] At -0.3 V vs. RHE and pH 14 (1 M KOH for the electrolyte), which corresponds to a low 200 mV overpotential,

a high current density with j_{CO} = 22.2 mA/cm^2 was achieved (j_{CO} is the partial current density for CO production). The dependence of the current density for CO production is reported in Figure 15a (see also Figure 22). Upon setting the electrolysis potential at -0.72 V vs. RHE, j_{CO} raised to 111.6 mA/cm^2 with 96% selectivity, while excellent stability over the course of the 3h electrolysis was obtained (Figure 15b). The only additional gas phase by-product was H_2 (4% selectivity) and the catholyte solution was carefully checked by ^{1}H NMR; no formate nor methanol was detected during the experiment. The obtained j_{CO} corresponds to a turnover frequency (TOF) of 2.7 s^{-1} and a turnover number (TON) of 29008. A maximum current density of 165 mA cm^{-2} for CO generation was obtained at -0.92 V vs. RHE. Long term stability of the catalytic material was assessed upon applying a constant current density of 75 mA cm^{-2} for 10h, which led to a cathodic potential of -0.65 V vs. RHE (h = 540 mV) with 94% selectivity of CO (j_{CO} = 70.5 mA cm^{-2}) (Figure 23). All the collected data are compiled in Table 3, along with a comparison of previously reported catalysts. The type of cell used (H cell vs. flow cell) is also indicated to ease comparison between data. The Co K-edge XANES spectra of **CoPc2@**carbon black were recorded before and after electrocatalysis at *E*= -0.72 V vs. RHE. Figure 15c shows these spectra together with that of the starting **CoPc2** complex. All these spectra present the typical features expected for a cobalt(II) phthalocyanine complex, *i.e.* a low intensity pre-edge peak at 7111 eV (corresponding to a 1s to 3d/4p transition) and a shoulder at 7717 eV (corresponding to a 1s to 4p_z transition). Interestingly, the intensity of these two transitions were shown by Li *et al* [17] to depend on the attachment to a surface, *i.e.* the pre-edge intensity increases and the shoulder decreases upon adsorption onto nanotubes, respectively. The same trend is observed in the **CoPc2@**carbon black system, with decreased pre-edge and increased shoulder intensities on going from the starting complex to the adsorbed species. This trend continues after catalysis, suggesting an even closer interaction with the surface while maintaining the overall structure of the molecular catalyst after the experiment. This structural conservation is further confirmed by the EXAFS spectra (Figure 24), which also present the typical features of a cobalt phthalocyanine complex.[38] In addition, comparison of the spectrum of **CoPc2@**carbon black recorded after catalysis with those of reference cobalt samples (Figure 24) clearly shows that the changes observed on the spectrum after catalysis are insignificant as far as the overall structure is concerned.

[0055] Remarkably, **CoPc2** remains highly selective for the CO_2-to-CO conversion across an interval of 10 units of pH, extending from acidic (pH 4) to basic solutions (pH 14). An averaged 92% selectivity for CO_2 reduction with partial current density of ca. 20 mA cm^{-2} were routinely obtained in the whole domain of pH values with excellent stability over time. In close to neutral solutions (pH 7.3), **CoPc2** is a significantly better catalyst than the non-substituted phthalocyanine **CoPc** (see Table 3, entries 2 and 3) with a ca. 25% increase in current density at similar overpotential, but it also surpasses state-of-the art tetra-cyano substituted phthalocyanine (CoPc-CN, Table 3, entry 4) and unsubstituted Co phthalocyanine polymerized around carbon nanotubes (CoPpc, Table 3, entry 5), both in terms of current density and turnover frequency. Similarly to the previously reported cobalt phthalocyanines mentioned above, **CoPc2** exhibits excellent stability over time, showing a 10.5 h electrolysis experiment, with no loss of performance.

Table 3. Comparison of electrolysis performances between **CoPc2@**carbon powder hybrid catalyst and previously reported state-of-the art immobilized molecular Co catalysts and Ag nanomaterial.

Entry	Catalyst	*E* (V vs. RHE) [overpotential (mV)]	Electrolyte	*j*CO (mA cm^{-2})	TOF (s^{-1})	CO sel. (%)	Cell type	Ref.
1	**CoPc2**	-0.97 [836][a]	0.5 M KCl	16.3	6.1	92	H-cell	this work
2	**CoPc2**	-0.67$_5$ [539][a]	0.5 M $NaHCO_3$	18.1	6.8	93	H-cell	this work
3	**CoPc**	-0.67$_5$ [546][a]	0.5 M $NaHCO_3$	13.1	4.1	92	H-cell	this work
4	CoPc-CN	-0.63 [520]	0.1 M $KHCO_3$	14.7	4.1	98	H-cell	15
5	CoPpc	-0.61 [500]	0.5 M $NaHCO_3$	18	1.4	ca. 90	H-cell	16
6	Coqpy	-0.55 [440]	0.5 M $NaHCO_3$	19.9	12	99	H-cell	10
7	**CoPc2**	-0.31 [200][b]	1 M KOH	22.2	0.54	93	Flow-cell	this work

(continued)

Entry	Catalyst	*E* (V vs. RHE) [overpotential (mV)]	Electrolyte	*j*CO (mA cm^{-2})	TOF (s^{-1})	CO sel. (%)	Cell type	Ref.
8	**CoPc2**	-0.65 [540][b]	1 M KOH	70.5	1.67	94	Flow-cell	this work
9	**CoPc2**	-0.72 [610][b]	1 M KOH	111.6	2.7	96	Flow-cell	this work
10	**CoPc2**	-0.92 [810][b]	1 M KOH	165	3.9	94	Flow-cell	this work
11	CoPc-CN	-0.66 [550]	1 M KOH	31	/	94	Flow-cell	11
12	Ag[c]	-0.81 [700]	1 M KOH	156.5	/	92	Flow-cell	13

Entry 1: Γ = 14.4 nmol cm^{-2} (pH 4, 2h electrolysis), entry 2: Γ = 14.4 nmol cm^{-2} (pH 7.3, 1h electrolysis), entry 3: Γ = 23.3 nmol cm^{-2} (pH 7.3, 1h electrolysis), entries 7-10: Γ = 0.216 μmol cm^{-2} (pH 14, for 0.5, 10, 3 and 0.3 h electrolysis respectively). Typical uncertainty on j_{CO} and TOF values is ±5%.
[a]corrected from ohmic drop (uncompensated solution resistance of ca. 3 W, electrode surface 0.5 cm^2)
[b]uncorrected from ohmic drop
[c]carbonate-derived Ag nano-catalyst (500 nm thickness), see reference 13 for details.

[0056] A turnover frequency up to 6.8 s^{-1} was reached and, generally, a very small loading of the catalysts was necessary to obtain high j_{CO} (see for example Table 3, entries 1-2). Long term electrolysis (10h) in basic conditions (pH 14) at -0.65 V vs. RHE led to an average j_{CO} close 70.5 $mAcm^{-2}$ and also illustrates the remarkable stability of the cobalt catalyst. The ability to implement **CoPc2** in various pH conditions is also a key feature that may allow for combining the Co catalyst to various types of anodic materials in order to decrease the overall cell potential. In particular, the excellent performance obtained at pH 14 should permit to pair the **CoPc2** loaded cathode 9 with the most efficient oxygen evolving metal oxide anode 2 materials. At this pH, **CoPc2** matches the state-of-the art Ag based catalyst sputtered onto a PTFE membrane, both in terms of selectivity and current density (Table 3, compare entries 10 and 12).

[0057] Upon introducing a positively charged trimethylammonium group on the parent cobalt phthalocyanine, a highly efficient and versatile catalyst for the CO_2-to-CO electrochemical conversion in water has been obtained. Furthermore, it operates with high selectivity (92 to 96%) in a broad range of pHs, extending from acidic (pH 4) to basic conditions (pH 14). In acid and neutral conditions, current densities close to 20 mA cm^{-2} were routinely obtained. In a 1 M KOH electrolyte solution, same current densities could be obtained at a very low overpotential of 200 mV, once the hybrid catalyst mixed with carbon support was included in a gas flow cell. At -0.92 V vs. RHE, a partial current for CO production of 165 $mAcm^{-2}$ was found with 94% catalytic selectivity. These performances show that hybrid catalytic materials including only carbon and an earth abundant metal based molecular complex can rival noble metal nanomaterials such as Ag and Au. This study highlights that rational tuning of the structure of simple metal complexes may allow for high performance, and it is likely that further improvement is yet to come. Finally, this work opens new perspectives for the development of low-cost catalytic materials to be included in CO_2 electrolysers.

Supplementary Information

Methods

[0058] All electrocatalytic reactions were carried out under an atmosphere of argon or CO_2. Chemicals, including **CoPc1** and supporting electrolytes were obtained from commercial suppliers. Supplementary Information section describes the synthesis and characterization of **CoPc2** and **FeTNT**, as well as typical protocols for electrocatalytic CO_2 reduction.

[0059] **Typical protocol for electrocatalytic CO_2 reduction**. After preparation of a catalytic ink containing either **FeTNT**, **CoPc1** or **CoPc2**, and deposition of the material onto porous carbon paper, controlled potential electrolysis were performed either in a closed electrochemical cell or in a flow cell electrolyser using a PARSTAT 4000 potentiostat (Princeton Applied Research). Gas chromatography analyses of gas evolved in the headspace during the electrolysis were performed with an Agilent Technologies 7820A GC system equipped with a thermal conductivity detector. Conditions

allowed detection of both H_2, O_2, N_2, CO, and CO_2. Calibration curves for H_2 and CO were determined separately by injecting known quantities of pure gas

General Considerations

Chemicals and characterization methods

[0060] Chemicals and materials were purchased from Sigma-Aldrich, Fluka, TCI America, ABCR or Alfa Aesar, and used as received. All aqueous solutions were prepared with Millipore water (18.2 MΩ cm). The MWCNTs were purchased from Sigma-Aldrich (O.D. × L 6-9 nm × 5 μm, > 95%). The cobalt (II) phthalocyanine (**CoPc1**) (β-form, dye content 97%) was purchased from Sigma-Aldrich. Toray Carbon Paper (CAS Number: 7782-42-5), TGP-H-60, 19x19cm was purchased from Alfa Aesar and used for preparation of the cathode 9s for the electrochemical cell. The cathode 9s (gas diffusion electrodes) used in the flow cell were prepared using Freudenberg C24H5 carbon paper (21 x 29.7 cm, product code F5GDL). VULCAN® XC72R Speciality Carbon Black was purchased from Cabot Corporation.

[0061] 4-*tert*-butylphthalonitrile was obtained from TCI America. 3-nitrophthalonitrile was purchased from ABCR. All solvents were of synthetic grade. Infrared spectra (IR) were recorded on a Bio-Rad FTS 175C FTIR spectrophotometer. UV-visible absorption spectra were obtained using a Shimadzu 2001 UV spectrophotometer. High resolution mass spectra were measured on an Agilent 6530 Accurate-Mass Q-TOF LC/MS spectrometer equipped with electrospray ionization (ESI) source. NMR spectra were recorded in deuterated chloroform ($CDCl_3$) and THF-d_8 on a Varian 500 MHz spectrometer. Melting points were recorded on a Stuart SMP apparatus.

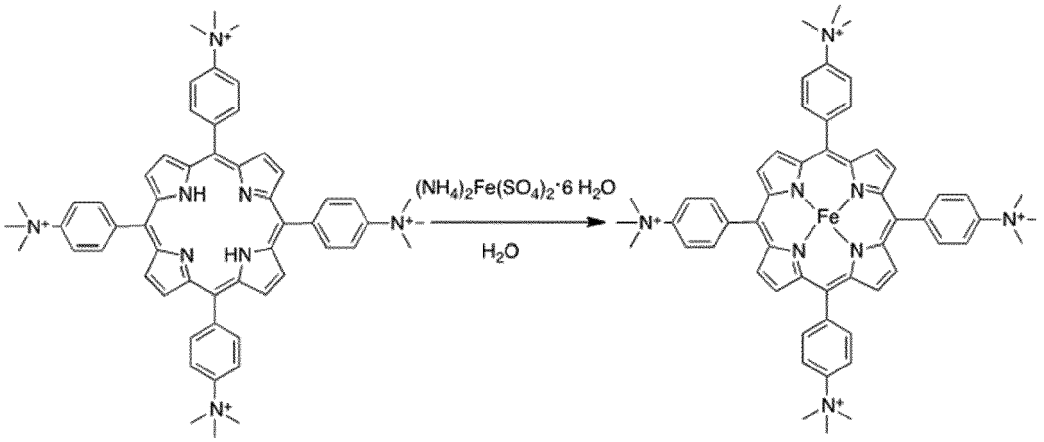

Synthesis of FeTNT

[0062] A solution of 5,10,15,20-tetrakis(4-trimethylammoniophenyl)porphyrin tetrachloride (250 mg, 0.253 mmol, 1 eq) in water (500 mL) is prepared and put under argon flux, Mohr's salt is added to the solution (810 mg, 3.75 mmol, 15 eq) and the solution is heated to 85°C for 4 h. Ammonium hexafluorophosphate (2.5 g, 15 mmol, 60 eq) is added and the obtained precipitate is separated by centrifugation (10000 rpm, 30 min). The red solid obtained is rinsed one time in pure water and separated again by centrifugation (10000 rpm 30 min), then rinsed one time in 1 to 1 mixture of chloroform and acetone and separated by centrifugation (10 000 rpm 30 min). Residual solvent is evaporated under Argon flux. Yield: 92 % (343 mg)

UV-Vis (DMF): λ_{max} nm (log ε) 407 (4), 568 (4.98).

[0063] Cobalt catalyst **CoPc2** was prepared as illustrated here:

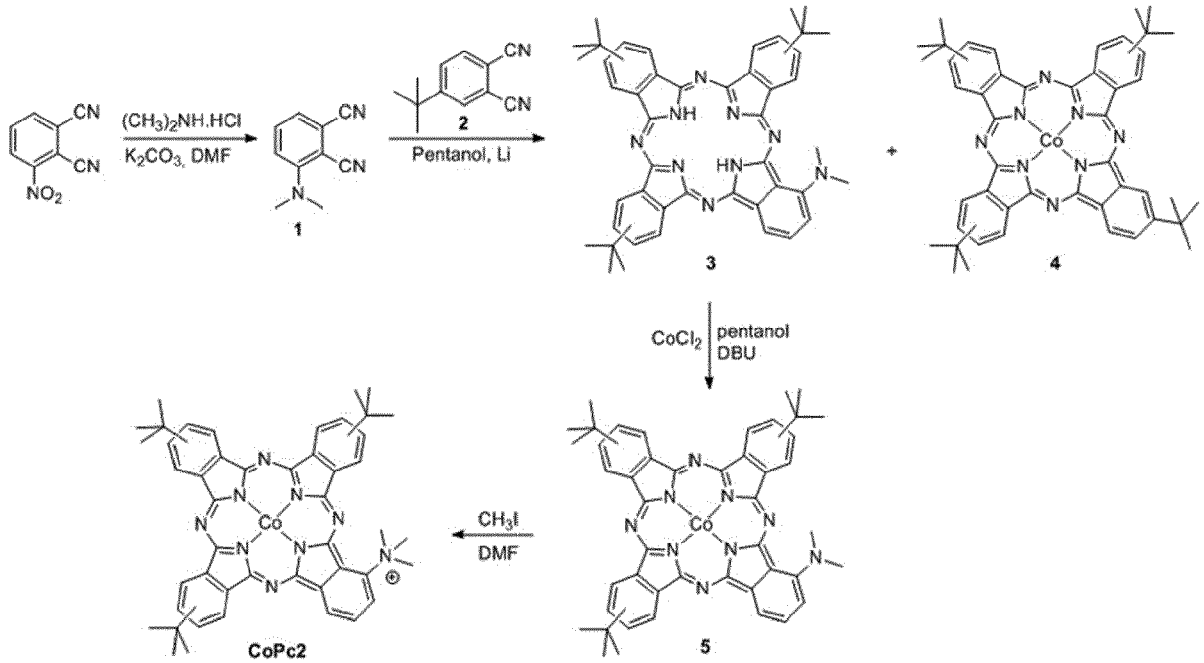

Synthesis of phthalonitrile and phthalocyanines.

Synthesis of 3-(dimethylamino)phthalonitrile **1**

[0064] 3-Nitrophthalonitrile (2 g, 11.5 mmol) and dimethylamine hydrochloride (2.8 g, 34.6 mmol) were dissolved in anhydrous DMF (30 mL) under argon atmosphere then finely powdered dry potassium carbonate (30 g, 217.5 mmol) was added portion-wise over 15 min. The reaction mixture was stirred under argon at 65 °C for 24 h then poured into water (250 mL). The resulting solid was collected by filtration and washed with water. After drying in vacuum, the crude product was recrystallized from ethanol. Yield: 80 % (1.57 g). m.p. 105 °C. ^{1}H NMR (500 MHz, $CDCl_3$): δ, ppm 3.18 (s, 6H), 7.12 (d, 1H), 7.15 (d, 1H), 7.46 (t, 1H). ^{13}C NMR (125 MHz, $CDCl_3$): δ, ppm 172.4, 155.4, 133.1, 123.0, 120.5, 118.0, 116.6, 116.3, 110.0, 100.6, 42.7. FT-IR (v, cm^{-1}): 2992, 2937, 2874, 2203, 1584, 1486, 1425, 1357, 1244, 1192, 1122, 1008, 792, 722.

Synthesis of phthalocyanine **3**

[0065] Granules of lithium were added to anhydrous *n*-pentanol (10 mL). This mixture was heated to 60 °C under argon flux until total consumption of the granules. 3-(dimethylamino)phthalonitrile **1** (0.25 g, 1.46 mmol) and 4-*tert*-butylphthalonitrile **2** (3.2 g, 17.52 mmol) were then added and this reaction mixture was refluxed for 18 h, then cooled to room temperature and poured to an ethanol/water mixture. The resulting dark blue-green precipitate was filtered off, washed several times with water and dried. Phthalocyanine **3** was isolated from this crude mixture of phthalocyanines by chromatography on silica gel using a mixture of CH_2Cl_2/EtOH (100:1) as the eluent. The tetra-*tert*-butylphthalocyanine **4** was first eluted and the phthalocyanine **3** was the second eluted compound. Yield: 15 % (160 mg). ^{1}H NMR (500 MHz, THF-d_8): δ, ppm -2.04 (s, 1H), -1.95 (s, 1H), 1.84 (m, 10H), 1.88-1.94 (m, 17H), 3.70 (s, 3H), 7.45 (d, 1H), 7.79 (m, 1H), 8.10-8.40 (m, 4H), 8.61 (d, 1H), 8.85-8.91 (m, 1H), 8.98- 9.24 (m, 4H), ^{13}C NMR (125 MHz, THF-ds): δ, ppm 152.97, 152.94, 152.88, 152.84, 152.61, 152.58, 150.16, 150.12, 133.67, 129.92, 127.43,127.30, 127.22, 126.75, 125.50,122.12, 122.07, 121.93, 121.90, 121.77, 118.69, 118.65, 118.51, 118.48, 118.41, 117.87, 117.83, 114.74, 78.54, 78.28, 78.02, 44.36, 39.98, 37.15, 37.06, 35.67, 35.60, 35.50, 31.89, 31.43, 31.32, 29.65, 29.32, 22.58, 13.43. ESI-HRMS: m/z 726.4030 $[M]^+$ calculated for $C_{46}H_{47}N_9$: 725.95. UV-vis (DMF): λ_{max} nm (log ε) 346 (3.90), 689 (4.87), 718 (5.38). FT-IR (v, cm^{-1}): 3288, 2955, 2863, 2776, 1618, 1501, 1316, 1186, 1014, 828, 742.

Synthesis of phthalocyanine **5**

[0066] A mixture of phthalocyanine **3** (50 mg, 0.06 mmol), $CoCl_2$ (18 mg, 0.12 mmol), and DBU (1 mL) in dried *n*-pentanol (5 mL) was heated to reflux for 18 h under argon. After cooling to room temperature, the reaction mixture was poured into an ethanol/water mixture. The resulting precipitate was filtered off and washed several times with water.

Phthalocyanine **5** was purified by chromatography on silica gel using a mixture of CH_2Cl_2/EtOH (50:1) as the eluent. Yield: 75 % (35 mg). ESI-HRMS: m/z 782.3234 $[M]^+$ calculated for $C_{46}H_{45}CoN_9$: 782.86. UV-vis (DMF): λ_{max} nm (log ε) 332 (3.70), 693 (4.74); FT-IR (v, cm^{-1}): 2955, 2856, 1606, 1457, 1316, 1254, 1094, 804, 737.

Synthesis of phthalocyanine **CoPc2**

[0067] Phthalocyanine 5 (35 mg, 0.044 mmol) was dissolved in DMF (5 mL), and methyl iodide (0.2 g, 1.5 mmol) was added. The mixture was stirred at room temperature for 16 h then poured into diethyl ether (25 mL). The resulting blue precipitate was filtered off, washed with ether and dried. Yield: 32 mg (88%). ESI-HRMS: m/z 797.3668 $[M]^+$ calculated for $C_{47}H_{48}CoN_9$: 797.90. Anal. calcd for $C_{47}H_{58}CoIN_9O_5$ ($CoPc2.5H_2O$): C, 55.28; H, 5.98; N, 11.88. Found: C, 55.62; H, 5.76; N, 12.42. UV-vis (DMF): λ_{max} nm (log ε) 326 (4.41), 664 (4.65). FT-IR (v, cm^{-1}) 3047, 2949, 2851, 1655, 1606, 1476, 1328, 1254, 1088, 933, 829, 749.

Preparation of the hybrid materials

[0068] For CV experiments and electrolysis in the closed electrolysis cell, 3 mg of MWCNTs were dispersed in 2 mL ethylene glycol (EG)/ethanol (EtOH) 1:1(v/v) mixture followed by 30 min of sonication. 1 mg of the cobalt catalyst (**CoPc1, CoPc2**) was dissolved in 1mL EG/EtOH mixture. Various volumes of this solution were added to the MWCNTs suspension in a total volume of 3 mL, so as to get mass ratio (1:6, 1:15 and 1:30) of the catalyst. The suspension was further sonicated for 30 min. Finally, Nafion® was added (2.9 %, 30 μL) and the complete mixture was sonicated for 30 min to obtain the final catalytic ink.

[0069] For the flow cell set-up, 3 mg of carbon black were dispersed in 3 mL EtOH followed by 30 min of sonication. 0.2 mg of **CoPc2** was dissolved in 1mL EtOH so as to get a mass ratio (1:15) of the catalyst. The suspension was further sonicated for 30 min. Finally, Nafion® was added (2.9 %, 30 μL) and the complete mixture was sonicated for 30 min to obtain the final catalytic ink. The ink was drop casted on carbon paper masked with a Teflon frame to obtain an electrode area of 1x1 cm^2.

Electrochemical studies

[0070] Controlled potential electrolyses were performed using a PARSTAT 4000 potentiostat (Princeton Applied Research).

Preparative Scale Electrolysis

[0071] In the closed cell, experiments were carried out in a cell using a Toray carbon paper as working electrode, and a SCE reference electrode closely positioned one from the other. The Pt grid counter electrode was separated from the cathodic compartment with a glass frit. The catalytic ink was dropped on one face of the Toray carbon paper cathode 9 (100 μL for a 0.5 cm^2 electrode), and allowed to dry under ambient conditions prior to use. The full cell setup was identical to the one used previously.[18]

[0072] The flow cell electrolyzer 1 (Micro Flow Cell® purchased by Electrocell) is composed by a sandwich of flow frames, electrodes, gaskets and a membrane, which, when assembled as illustrated in Figure 14, constitute a three-compartment flow cell. One compartment delivers the CO_2 (at 16.7 sccm) from the back side and through the gas diffusion electrode (GDE, 1x1 cm^2, fixated in a Pt frame), while another directs the catholyte solution (1 M KOH, flow rate of 16 sccm) in between the GDE and the anion exchange membrane 10 (AEM, Sustainion™ X37-50). On the other side of the latter, the anolyte (1 M KOH, flow rate of 16 sccm) is directed between the AEM and the Pt/Ti alloy anode 2. The flow frames are made of PTFE, and the gaskets of peroxide cured EDPM. Catholyte and anolyte were recycled using peristaltic pumps. All tubings were made of PTFE and connected to the cell with PEEK ferrules and fittings. The whole setup is schematically shown below (Figure 16).

Gas Detection

[0073] Gas chromatography analyses of gas sampled from the headspace during the electrolysis were performed with an Agilent Technologies 7820A GC system equipped with a thermal conductivity detector. CO and H_2 production was quantitatively detected using a CP-CarboPlot P7 capillary column (27.46 m in length and 25 μm internal diameter). Temperature was held at 150 °C for the detector and 34 °C for the oven. The carrier gas was argon flowing at 9.5 mL/min at constant pressure of 0.4 bars. Injection was performed via a 250-μL gas-tight (Hamilton) syringe previously degassed with CO_2. Conditions allowed detection of both H_2, O_2, N_2, CO, and CO_2. Calibration curves for H_2 and CO were determined separately by injecting known quantities of pure gas.

XPS analysis

[0074] An X-Ray Photoelectron Spectrometer THERMO-VG ESCALAB 250 (RX source K Al (1486.6 eV)) was used.

XAS data collection and analysis

[0075] X-ray absorption spectra (XAS) were collected at the LUCIA beamline of SOLEIL with a ring energy of 2.75 GeV and a current of 490 mA. The energy was monochromatized by means of a Si(111) double crystal monochromator. Data were collected in a primary vacuum chamber as fluorescence spectra with an outgoing angle of 5° using a Bruker silicon drift detector. The data were normalized to the intensity of the incoming incident energy and processed with the Athena software from the IFEFFIT package. For the EXAFS analysis, an E_0 value of 7722.0 eV was used for the cobalt K-edge jump energy.

SEM analysis

[0076] Scanning electron microscopy using a field emission gun (SEM-FEG) was performed using a Zeiss Supra 40.

THIRD EMBODIMENT

[0077] The inventors tested the cobalt quater pyridine (Co(qpy)) in the same cell as the first embodiment. Two types of experiments have been performed on the Co(qpy). The faradaic efficiency for CO has been measured chronopotentiometry at several current densities and the stability of the catalyst has been determined at 50 mA/cm^2.

[0078] During chronopotentiometry experiment the Co(qpy) showed faradaic efficiencies for CO higher than 90 % at current densities under 100 mA/cm^2. Then, at higher current densities, the faradaic efficiency for CO decreases drastically.

Cell potential (V)	j/mA.cm^{-2}	% CO
1.71	25	96.6
1.80	50	98.7
1.88	75	98.8
2.24	100	91.6
2.60	125	86.1
2.71	150	64.6
2.73	175	34.7
2.74	200	16.6

[0079] In figure 26, Co(qpy) can maintain at 50 mAcm^{-2} a faradaic efficiency higher than 90 % for CO for 12 hours. The decrease is steady until 24 hours of experiments. Then, the faradaic efficiency drops under 40 % for CO.

References

[0080]

1. Azcarate, I., Costentin, C., Robert, M., Savéant, J.-M. Through-space charge interaction substituent effects in molecular catalysis leading to the design of the most efficient catalyst of CO2-to-CO electrochemical conversion. J. Am. Chem. Soc. 138, 16639-16644 (2016*).*

2. Francke, R., Schille, B., Roemelt, M., Homogeneously catalyzed electroreduction of carbon dioxide-Methods, mechanisms, and catalysts. Chem. Rev. 116, 4631-4701 (2018*).*

3 Costentin, C., Robert, M., Savéant, J.-M. Catalysis of the electrochemical reduction of carbon dioxide. Chem. Soc. Rev. 42, 2423-2436 (2013*).*

4 Qiao, J., Liu, Y., Hong, F., Zhang, J. A review of catalysts for the electroreduction of carbon dioxide to produce low-carbon fuels. Chem. Soc. Rev. 43, 631-675 (2014*).*

5 Elgrishi, N., Chambers, M. B., Wang, X., Fontecave, M. Molecular polypyridine-based metal complexes as catalysts for the reduction of CO2. Chem. Soc. Rev. 46, 761-796 (2017*).*

6. Grice, K. A. Carbon dioxide reduction with homogenous early transition metal complexes: Opportunities and challenges for developing CO2 catalysis. Coord. Chem. Rev. 336, 78-95 (2017*).*
7. Grills, D. C., Ertem, M. Z, McKinnon, M., Ngo, K. T., Rochford, J. Mechanistic aspects of CO2 reduction catalysis with manganese-based molecular catalysts. Coord. Chem. Rev. 374, 173-217 (2018*).*
8. Loewen, N. D.,Neelakantan, T. V., Berben, L. A. Renewable formate from C-H bond formation with CO2: using iron carbonyl clusters as electrocatalysts. Acc. Chem. Res. 50, 2362-2370 (2017*).*
9. Takeda, H., Cometto, C., Ishitani, O., Robert, M. Electrons, photons, protons and earth abundant metal complexes for molecular catalysis of CO2 reduction. ACS Catal. 7, 70-88 (2017*).*
10. Wang, M., Chen, L., Lau, T-C., Robert, M. Hybrid Co quaterpyridine complex /carbon nanotube catalytic material for CO2 reduction in water. Angew. Chem. Int. Ed. 57, 7769-7773 (2018*).*
11. Xu, L., Wu, Y., Yuan, X., Huang, L., Wu, Z., Xuan, J., Wang, Y., Wang. H. High-Performance Electrochemical CO2 Reduction Cells Based on Non-noble Metal Catalysts. ACS Energy Lett. 3, 2527-2532 (2018*).*
12. Kutz, R. B., Chen, Q., Yang, H., Sajjad, S. D., Liu, Z., Masel, I. R. Sustainion imidazolium-functionalized polymers for carbon dioxide electrolysis. Energy Technol. 5, 929-936 (2017*).*
13. Dinh, C-T., Garcia de Arquer, F. P., Sinton, D., Sargent, E. H. High Rate, Selective, and Stable Electroreduction of CO2 to CO in Basic and Neutral Media. ACS Energy Lett. 3, 2835 - 2840 (2018*).*
14. Verma, S., Hamasaki, Y., Kim, C., Huang, W., Lu, S., Jhong, H-R. M., Gewirth, A. A., Fujigaya, T., Nakashima, N., Kenis, P. J. A. Insights into the low overpotential electroreduction of CO2 to CO on a supported gold catalyst in an alkaline flow electrolyzer. ACS Energy Lett. 3, 193 - 198 (2018*).*
15. Zhang, X., Wu, Z, Zhang, X., Li, L., Li, Y., Xu, H., Li, X., Yu, X., Zhang, Z., Liang, Y., Wang, H., Highly selective and active CO2 reduction electrocatalysts based on cobalt phthalocyanine/carbon nanotube hybrid structures. Nat. Commun. 8, 14675 (2017*).*
16. Han, N., Wang, Y., Ma, L. et al., Supported cobalt phthalocyanine for high-performance electrocatalytic CO2 reduction. Chem 3, 652-664 (2017*).*
17. Li, N., Lu, W., Pei K., Chen, W. Interfacial peroxidase-like catalytic activity of surface-immobilized cobalt phthalocyanine on multiwall carbon nanotubes RSC Advances, 5, 9374-9380 (2015*).*
18. Wang M., Chen L. G., Lau T.-C., and Robert M. A Hybrid Co Quaterpyridine Complex/Carbon Nanotube Catalytic Material for CO2 Reduction in Water, Angew. Chem. 130, 7895 -7899, (2018*).*

Claims

1. A flow cell electrolyzer (1) to electrochemically reduce a gas reactant comprising CO_2, into gaseous CO and gaseous H_2, with:

- an anodic compartment comprising:

  • an anode (2) with a current collector, and on the current collector, at least a catalyst to electrochemically oxidize H_2O to O_2,
  • an anodic electrolyte solution (3), at a controlled flow rate Q_a, comprising: a solvent, and an anodic electrolyte, the solvent being water,

- An anodic electrolyte solution inlet (4) and an anodic electrolyte solution outlet (5) connected to the anodic compartment, to circulate the anodic electrolyte solution (3);
- a cathodic compartment comprising:

  • a cathodic electrolyte solution (6), at a controlled flow rate Q_c, comprising: a solvent, and a cathodic electrolyte, the solvent being water,
  • a gas diffusion porous cathode (9) which comprises, on a gas diffusion porous current cathode collector which is electrochemically inert, at least a molecular catalyst incorporated in the porous cathode with a surface S, to electrochemically reduce the gas comprising CO_2 into gaseous CO, with a by-production of gaseous H_2,

the molecular catalyst being chosen between the list:

❖ metal porphyrin with one or several $+N(C_1\text{-}C_4$ alkyl$)_3$ groups, with the metal chosen among: Iron, Cobalt;
❖ metal phthalocyanine, with the metal chosen among: Iron, Cobalt;
❖ metal phthalocyanine with the metal chosen among: Iron, Cobalt, with one or several groups among:

$+N(C_1\text{-}C_4\ alkyl)_3$, F, $C(CH_3)_3$, or
❖ cobalt quater pyridine

- a channel (11) for flowing the reagent gas CO_2, at a controlled flow rate Q_g, onto or through the surface S of the gas diffusion porous current cathode collector;
- a cathodic electrolyte solution inlet (7) and a cathodic electrolyte solution outlet (8) connected to the cathodic compartment, to circulate the cathodic electrolyte solution, and the remaining reagent gas CO_2 and the product gas CO by the outlet (8);
- an anion exchange membrane (10), impermeable to CO_2, CO, H_2 and O_2, between the anodic compartment and the cathodic compartment;
- Pumping means (12) serving to:

  - Circulate by pumping the anodic electrolyte solution (3) and the cathodic electrolyte solution (6) between the inlet (4,7) and the outlet (5,8),
  - flow by pumping the comprising gas CO_2 passing through the gas diffusion porous cathode (9);

the pumping means being configured to control all flow rates of the cathodic and anodic electrolytes as well as the reagent gas CO_2 passing through the surface S of the gas diffusion porous cathode (9);

- a power supply providing the energy necessary to trigger the electrochemical reactions involving the reagent.

2. The flow cell electrolyzer (1) of claim 1, wherein the anodic and/or cathodic electrolyte solution has a neutral or basic pH.

3. The flow cell electrolyzer (1) of claim 1 or 2, wherein the anodic electrolyte solution and/or the cathodic electrolyte solution has a pH from 9 to 14, preferably from 10 to 14, more preferably from 11.5 to 14, and more preferably from 13 to 14.

4. The flow cell electrolyzer (1) of claims 1-3, wherein the molecular catalyst is the iron porphyrin with the formulae:

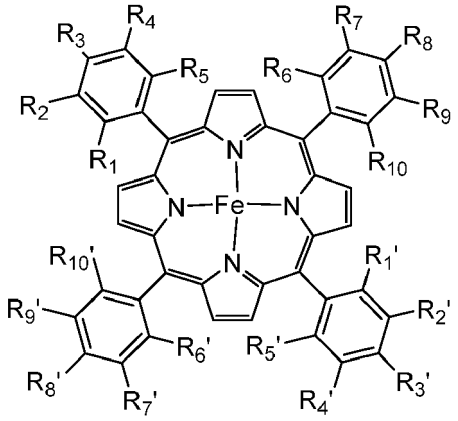

(I)

Wherein:

◦ at least 1 and at most 8 groups among R_1 to R_{10} and $R_{1'}$ to $R_{10'}$ being independently $+N(C_1\text{-}C_4\ alkyl)_3$ group,
◦ the other groups R_1 to R_{10} and $R_{1'}$ to $R_{10'}$ are independently selected from the group consisting of H, OH, F, $C(CH_3)_3$

5. The flow cell electrolyzer (1) of claim 4, wherein the iron molecular catalyst comprises:

- the other groups among R_1 to R_{10} and $R_{1'}$ to $R_{10'}$ are H; or

- the other groups among R_1 to R_{10} and $R_{1'}$ to $R_{10'}$ are H and F;

6. The flow cell electrolyzer (1) of claims 4-5, wherein the iron molecular catalyst comprises the $+N(C_1\text{-}C_4\ alkyl)_3$ groups in the para or ortho position.

7. The flow cell electrolyzer (1) of claims 1-3, wherein the molecular catalyst presents the formulae:

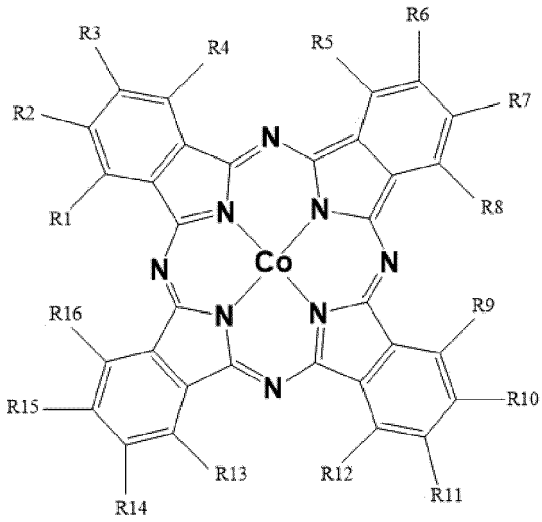

wherein R_1 to R_{16} are independently selected from the groups consisting of H, F $C(CH_3)_3$, or $+N(C_1\text{-}C_4\ alkyl)_3$

8. The flow cell electrolyzer (1) of claim 7, wherein R_1 to R_{16} are H.

9. The flow cell electrolyzer (1) of claim 7, wherein the cobalt molecular catalyst presents at least 1 and at most 8 groups among R_1 to R_{16} being independently $+N(C_1\text{-}C_4\ alkyl)_3$ group.

10. The flow cell electrolyzer (1) of claim 9, wherein the cobalt molecular catalyst presents for one or several of the specific following R_1, R_4, R_5, R_8, R_9, R_{12}, R_{13} and R_{16} groups, a $+N(C_1\text{-}C_4\ alkyl)_3$ substituent.

11. The flow cell electrolyzer (1) of any of claims 1-10, wherein the cathodic electrolyte comprises a phosphate buffer or potassium hydroxide, and the anodic electrolyte comprises a phosphate buffer or potassium hydroxide.

12. The flow cell electrolyzer (1) of any of claims 1-6, with the iron porphyrin as molecular catalyst, wherein:

- the pH is between 7.3 and 14
- the potential applied to the cathode 9 is between 0 V and -1 V versus RHE, and
- the current density for CO production is at least 150 $mAcm^{-2}$, and
- the selectivity of the electrochemical reaction is between 98% and 99.9%

13. The flow cell electrolyzer (1) of any of claims 7-8, with the phthalocyanine, wherein:

- the pH is between 7.3 and 14,
- the potential applied to the cathode 9 is between -0.48 V and -0.98 V versus RHE,
- the current density for CO production is at least 50 $mAcm^{-2}$,
- the selectivity of the electrochemical reaction is between 90% and 92%.

14. The flow cell electrolyzer (1) of any of claims 7, 9, with the cobalt phthalocyanine with one or several $+N(C_1\text{-}C_4\ alkyl)_3$ groups, wherein:

- the pH is between 7.3 and 14,
- the potential applied to the cathode 9 is between -0.3 V and -1 V versus RHE,
- the current density for CO production is at least 150 $mAcm^{-2}$,

- the selectivity of the electrochemical reaction is between 92 % and 96 %.

15. The flow cell electrolyzer (1) of claims 1-3, with the cobalt quater pyridine, wherein:

- the pH is between 7.3 and 14,
- the potential applied to the cathode 9 is between -0.6 V and -1 V versus RHE,
- the current density for CO production is at least 150 $mAcm^{-2}$,
- the selectivity of the electrochemical reaction is between 86.1 % and 98.8 %.

16. The flow cell electrolyzer (1) of any of claims 1-15, wherein the cathodic current collector is carbon paper.

17. The flow cell electrolyzer (1) of any of claims 1-16, wherein the porous cathode (9) comprises on the current collector, an electrode film which contains polymers with the molecular catalysts and wherein the electrode film is deposited or grafted on the current collector.

18. The flow cell electrolyzer (1) of claims 1-17, wherein pumping means (12) recirculate the anodic electrolyte solution (3) and the cathodic electrolyte solution (6).

Figure 1

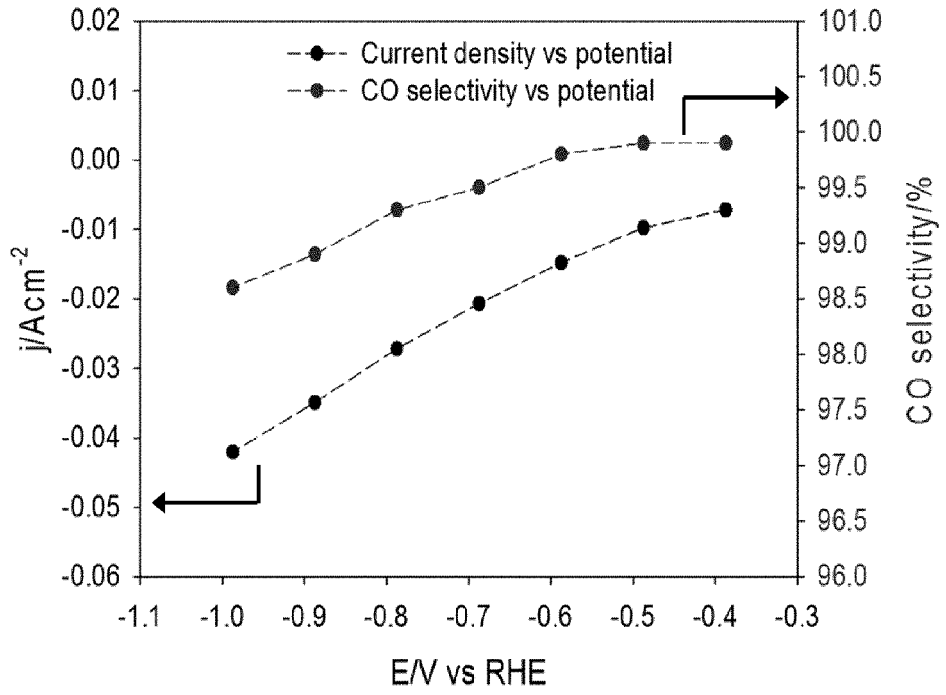

Figure 2

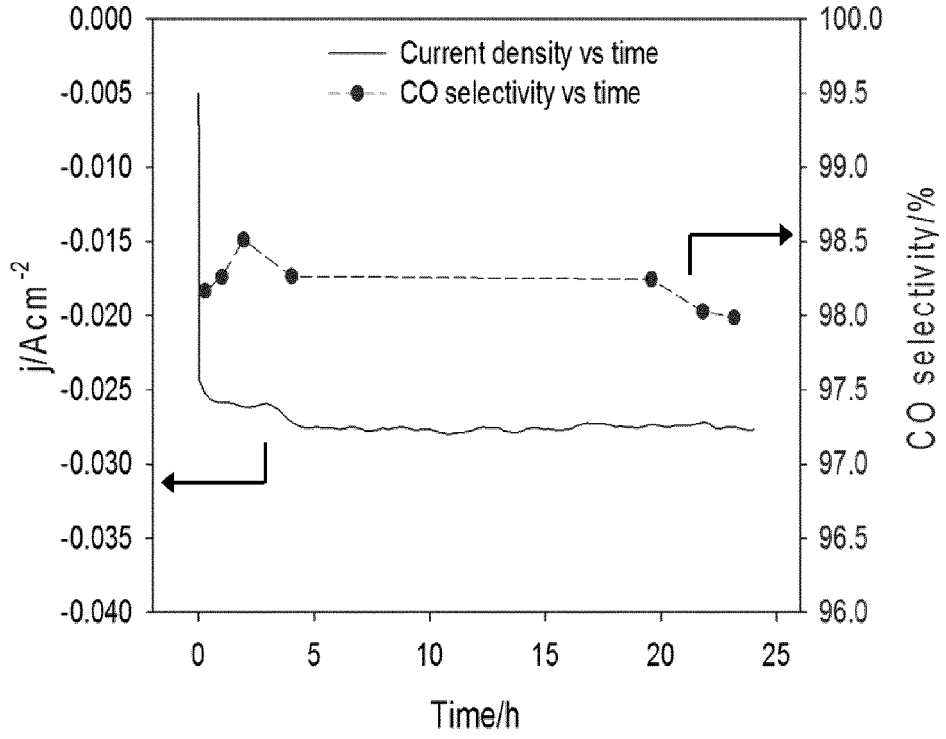

Figure 3

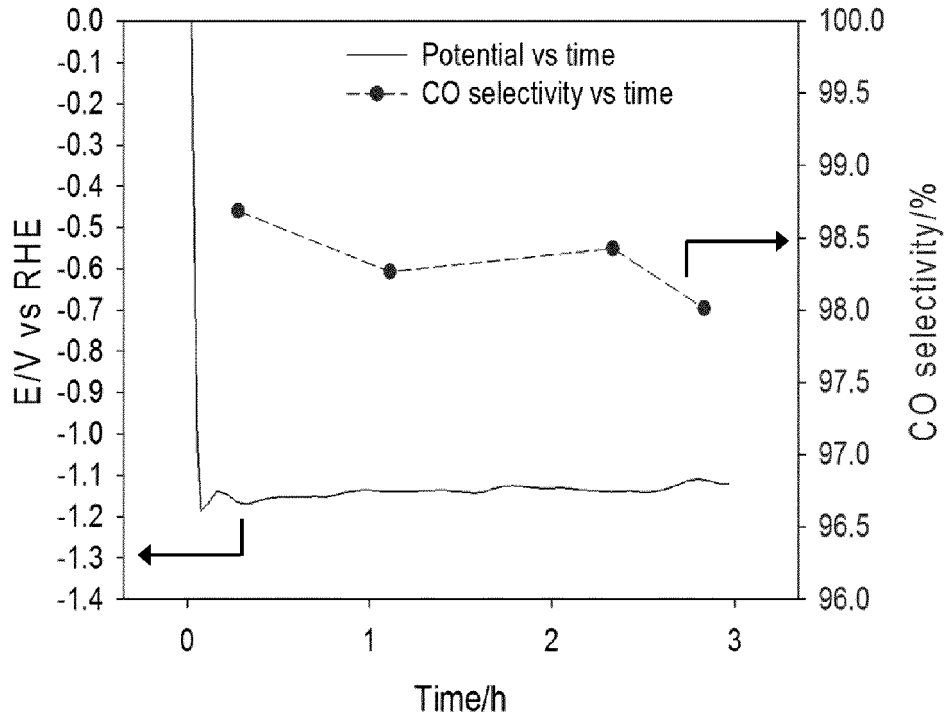

Figure 4

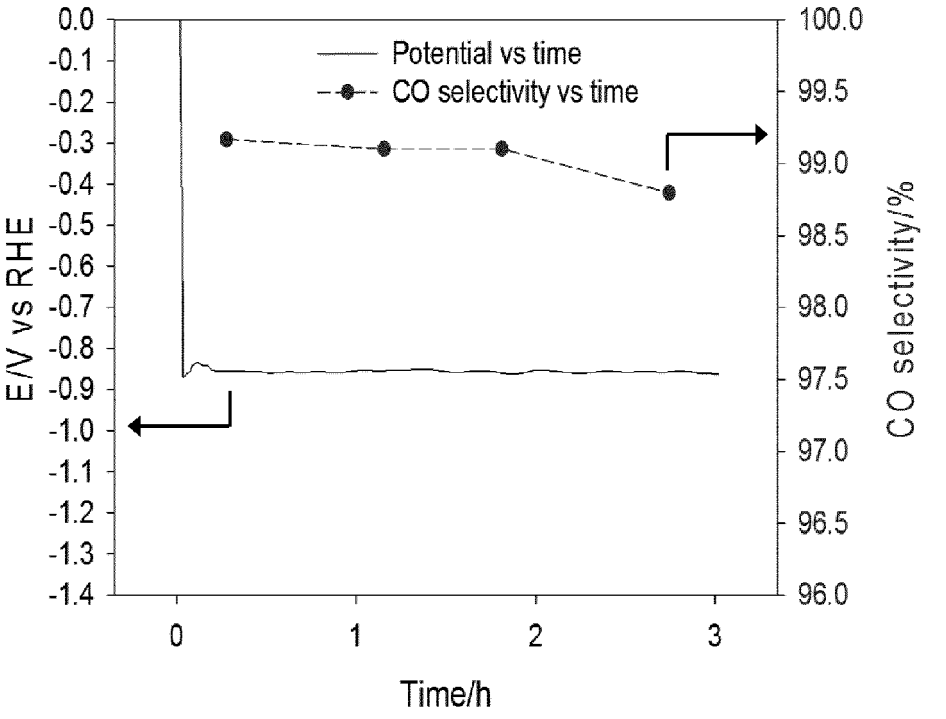

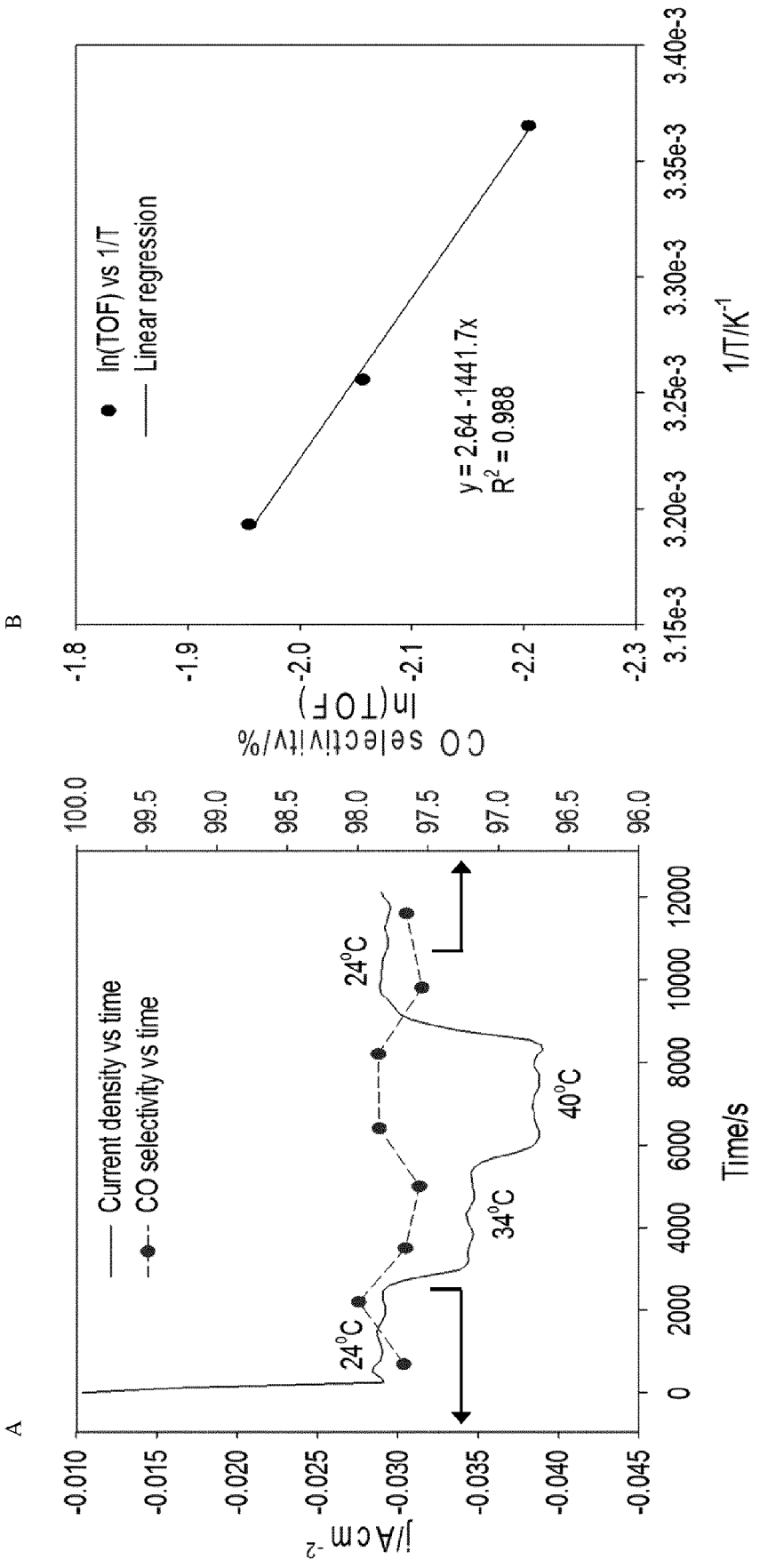
A
B
Current density vs time
CO selectivity vs time
24°C
34°C
40°C
24°C
j/A cm-2
CO selectivity/%
Time/s
ln(TOF)
1/T/K-1
ln(TOF) vs 1/T
Linear regression
y = 2.64 -1441.7x
R2 = 0.988

Figure 5

Figure 6

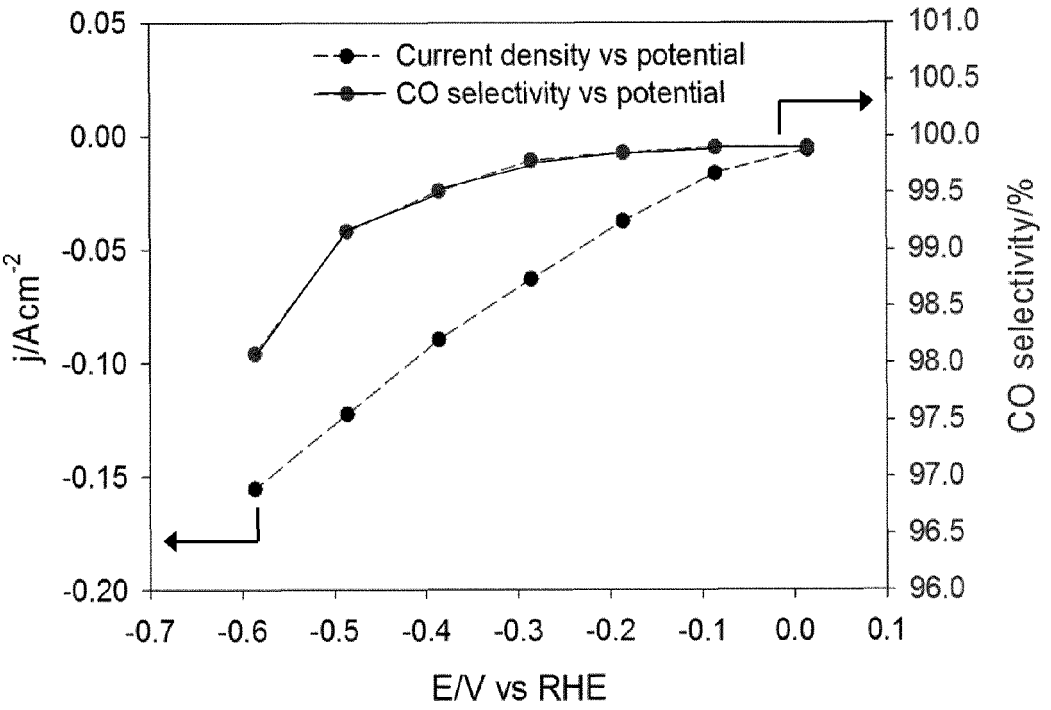

Figure 7

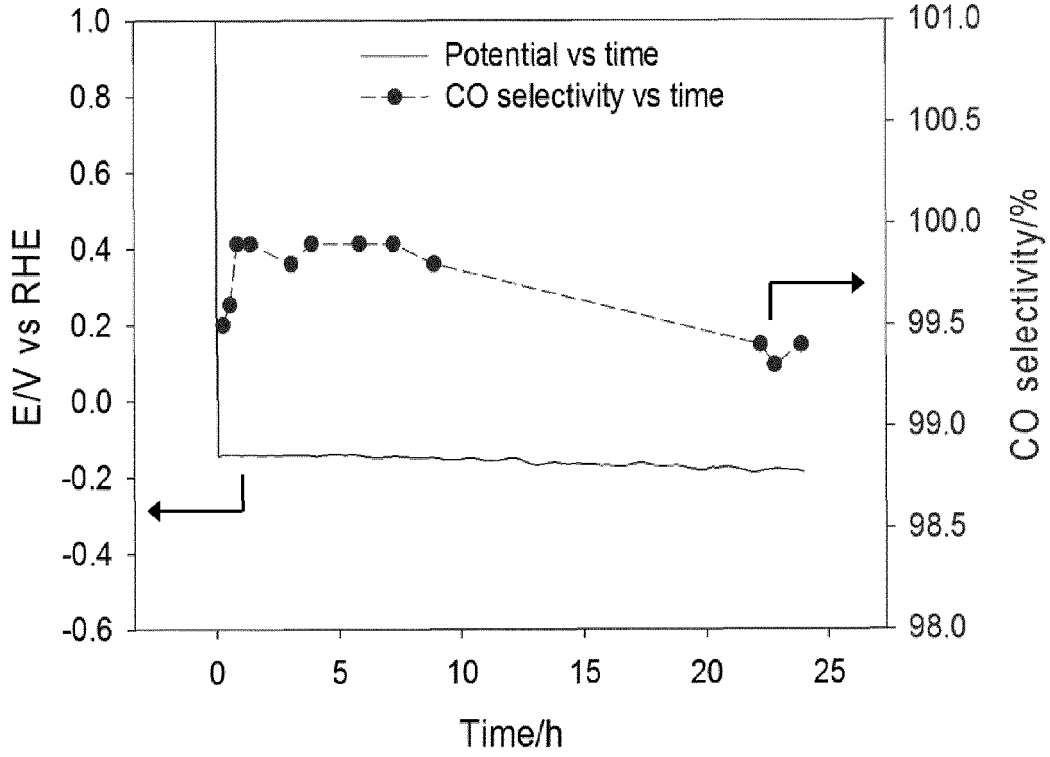

Figure 8

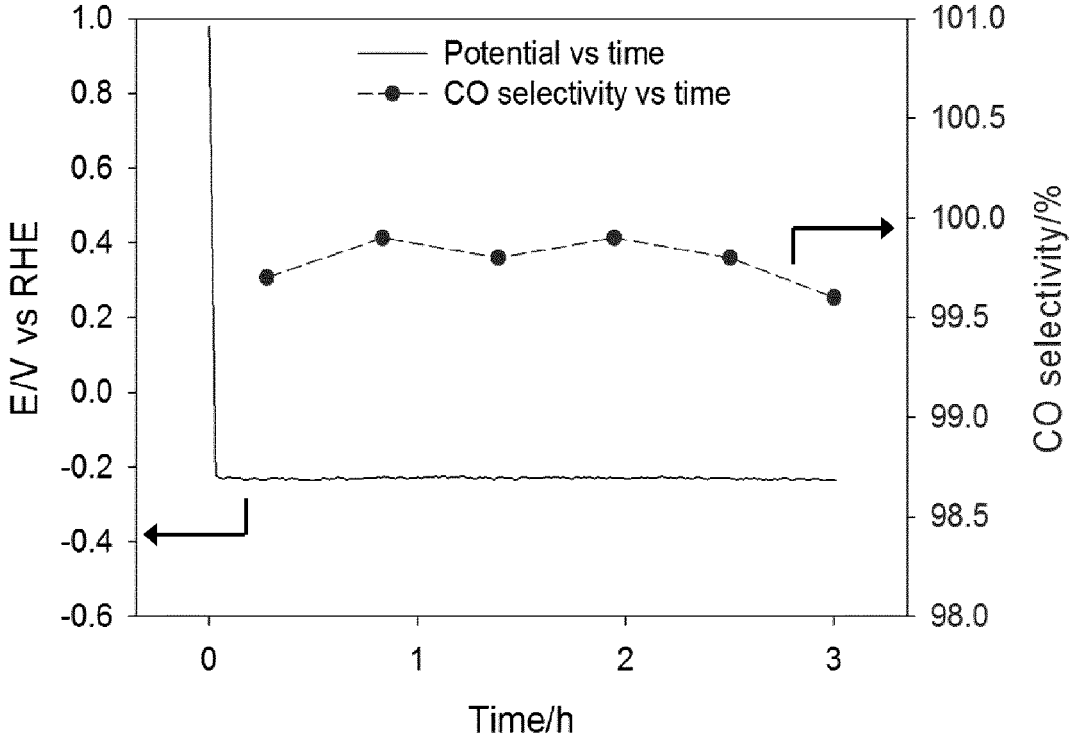

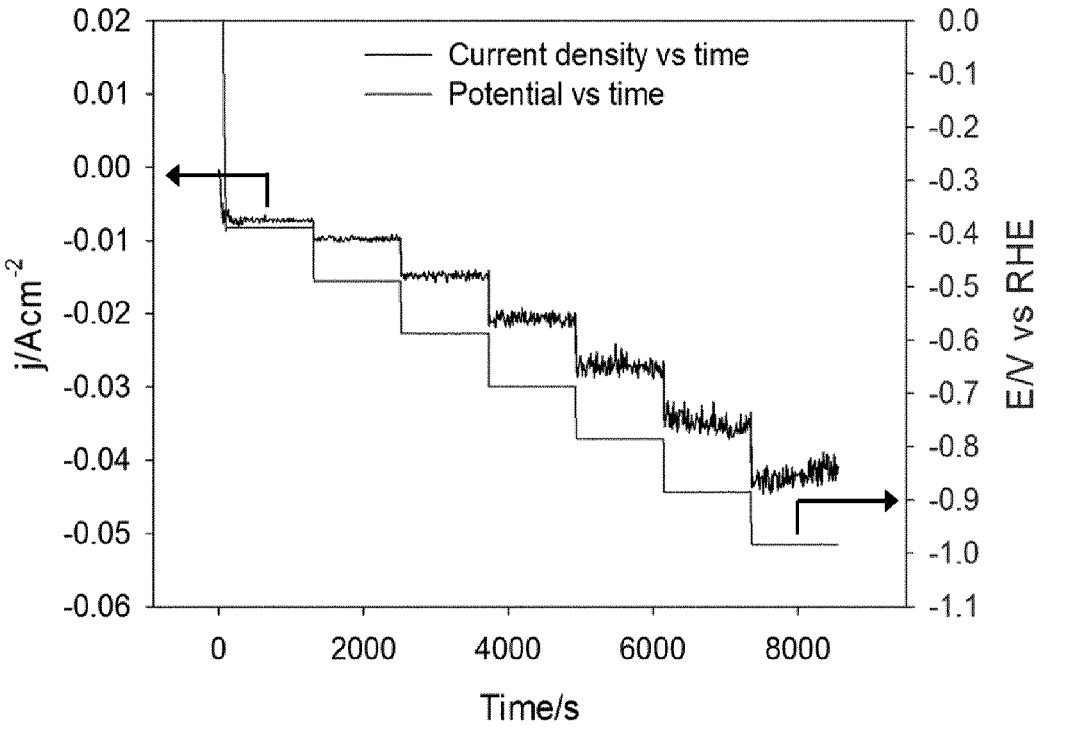

Figure 9

Figure 10

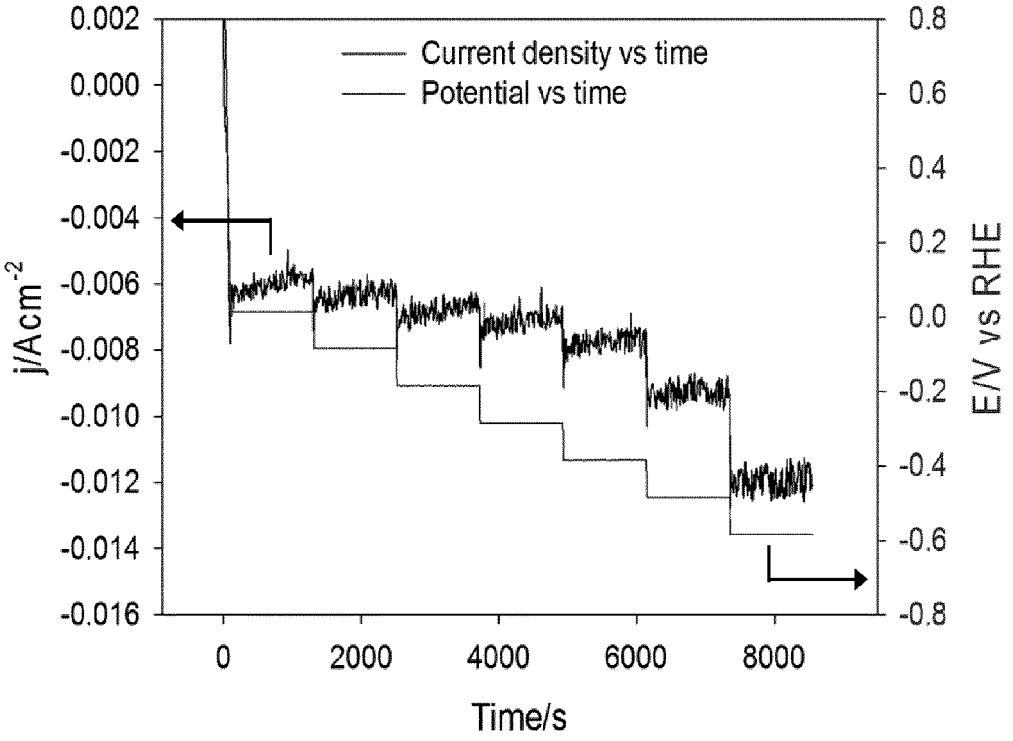

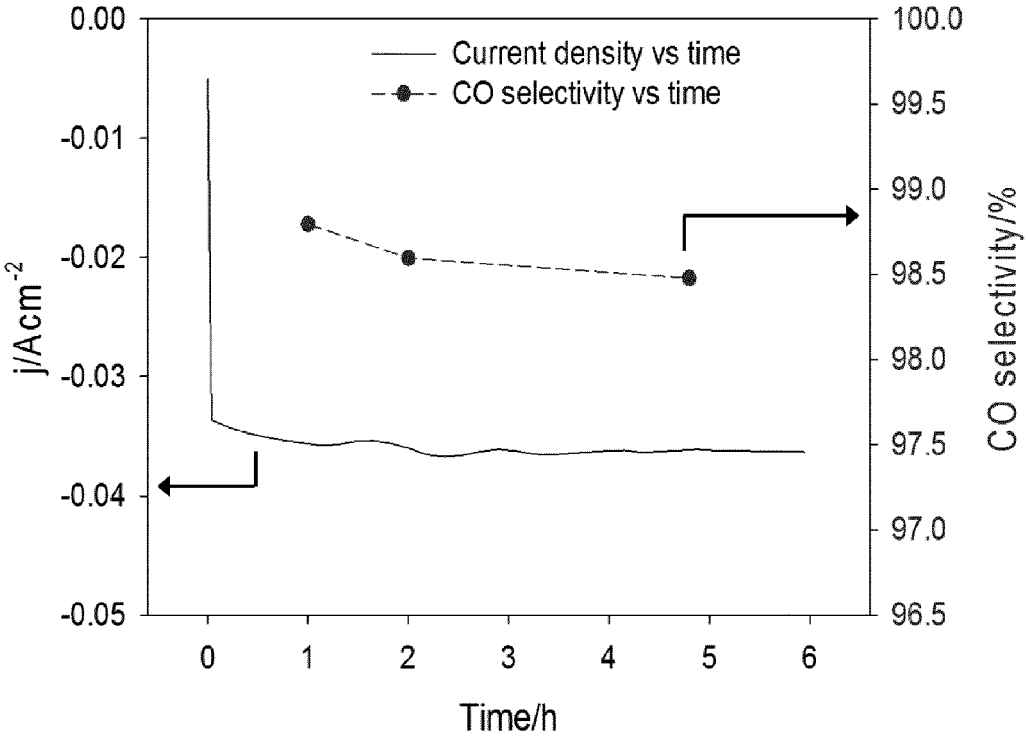

Figure 11

Figure 12

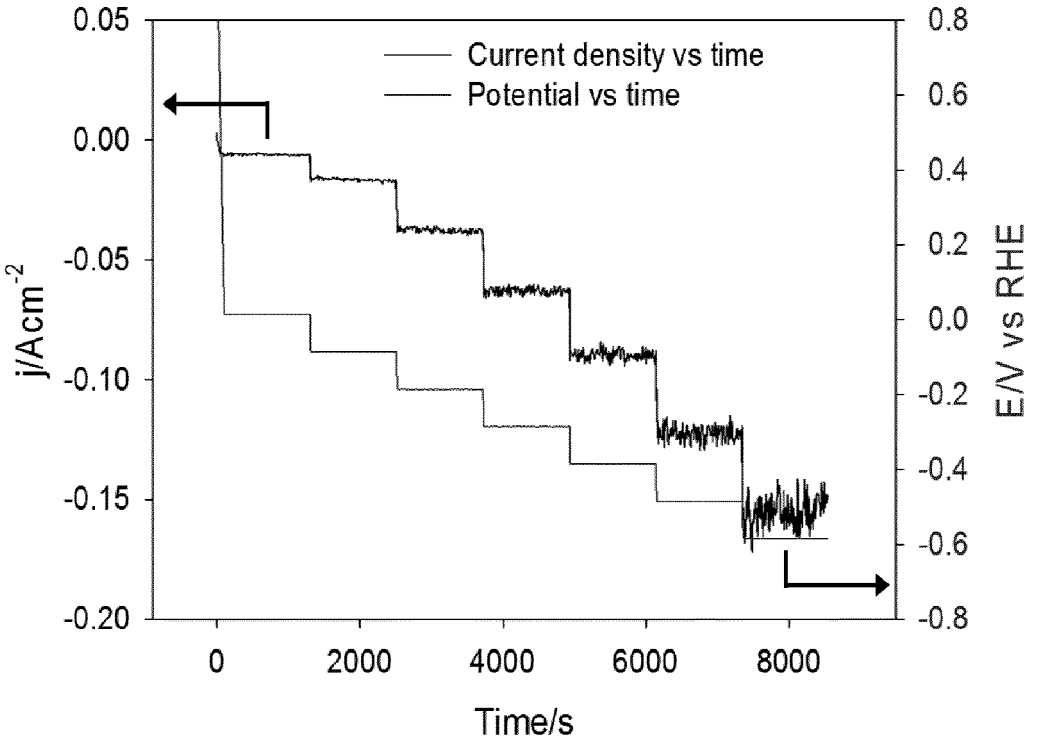

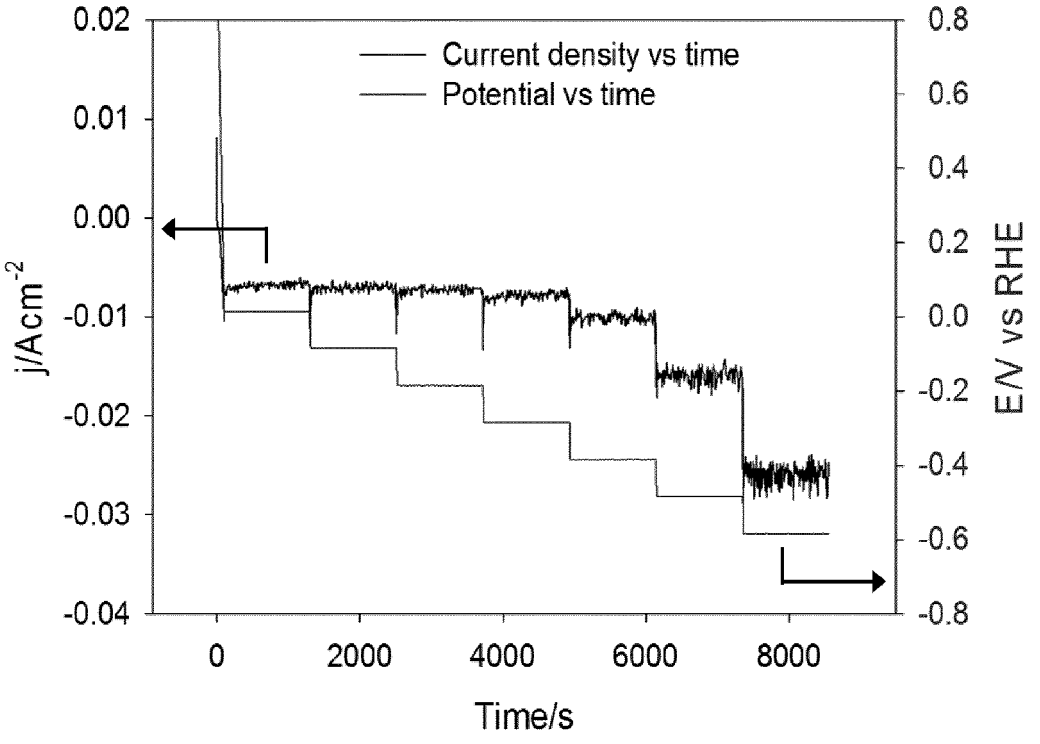

Figure 13

Figure 14

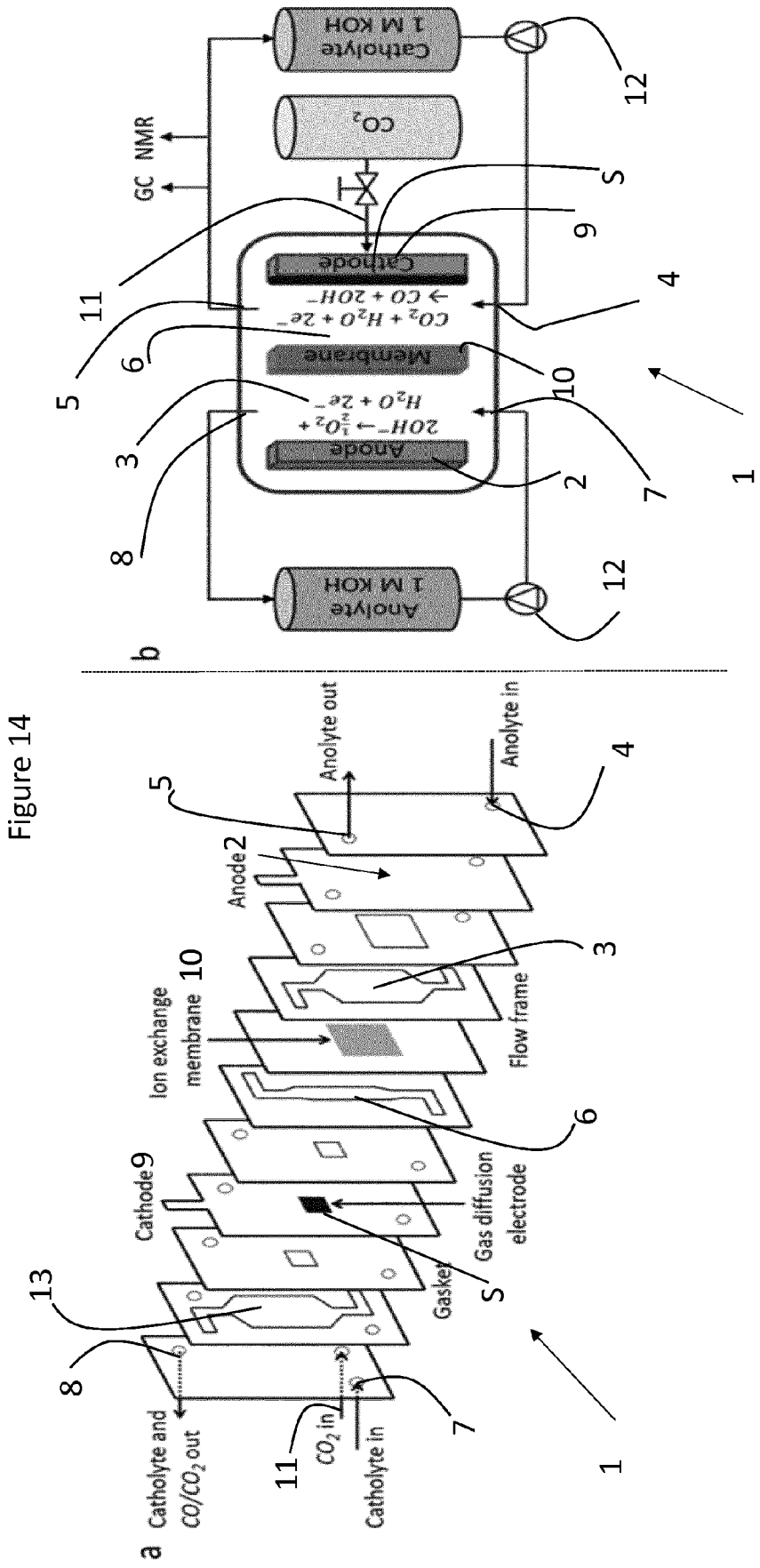
b
Anolyte
1 M KOH
Anode
Membrane
Cathode
Catholyte
1 M KOH
GC NMR
CO_2
$2OH^- \rightarrow \frac{1}{2}O_2 + H_2O + 2e^-$
$CO_2 + H_2O + 2e^- \rightarrow CO + 2OH^-$
a
Anolyte out
Anolyte in
Anode
Ion exchange membrane
Flow frame
Cathode
Gas diffusion electrode
Gasket
Catholyte and CO/CO_2 out
CO_2 in
Catholyte in

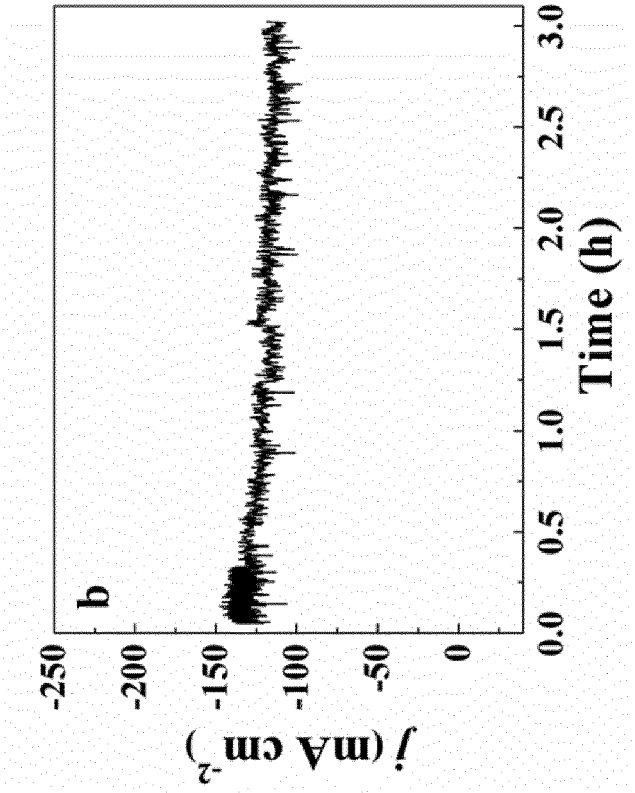

Figure 15b

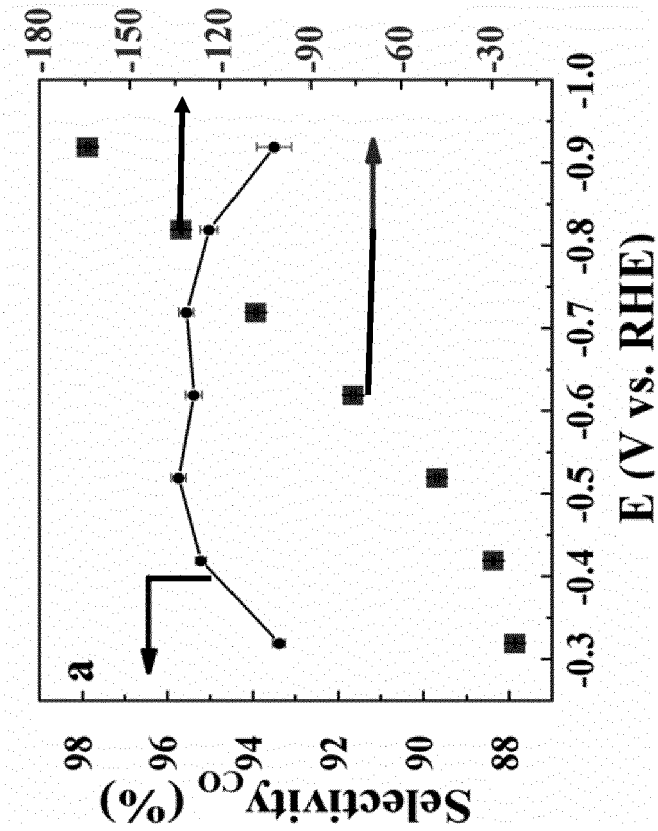

Figure 15a

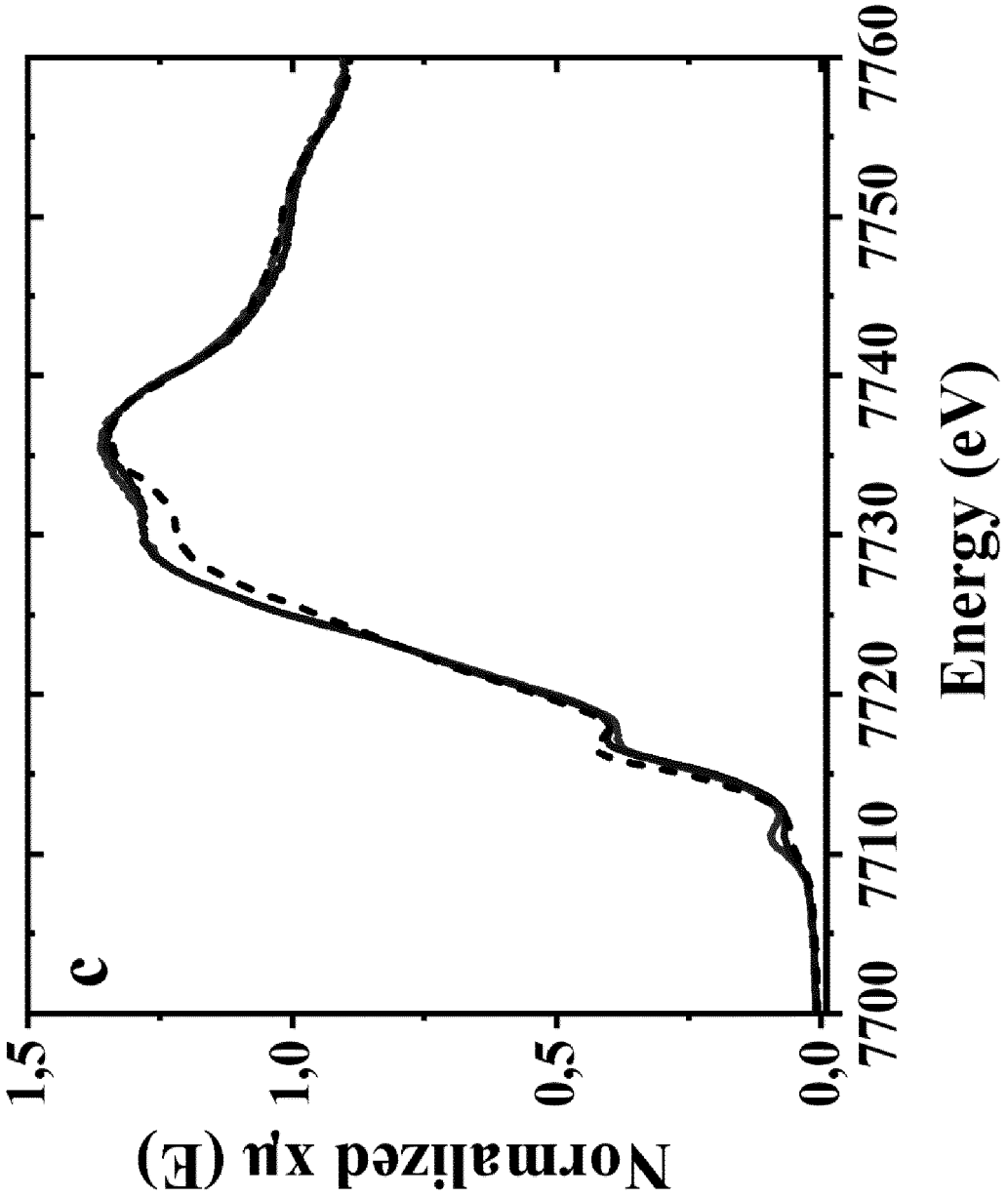
c
Normalized xμ (E)
1,5
1,0
0,5
0,0
7700
7710
7720
7730
7740
7750
7760
Energy (eV)

Figure 15c

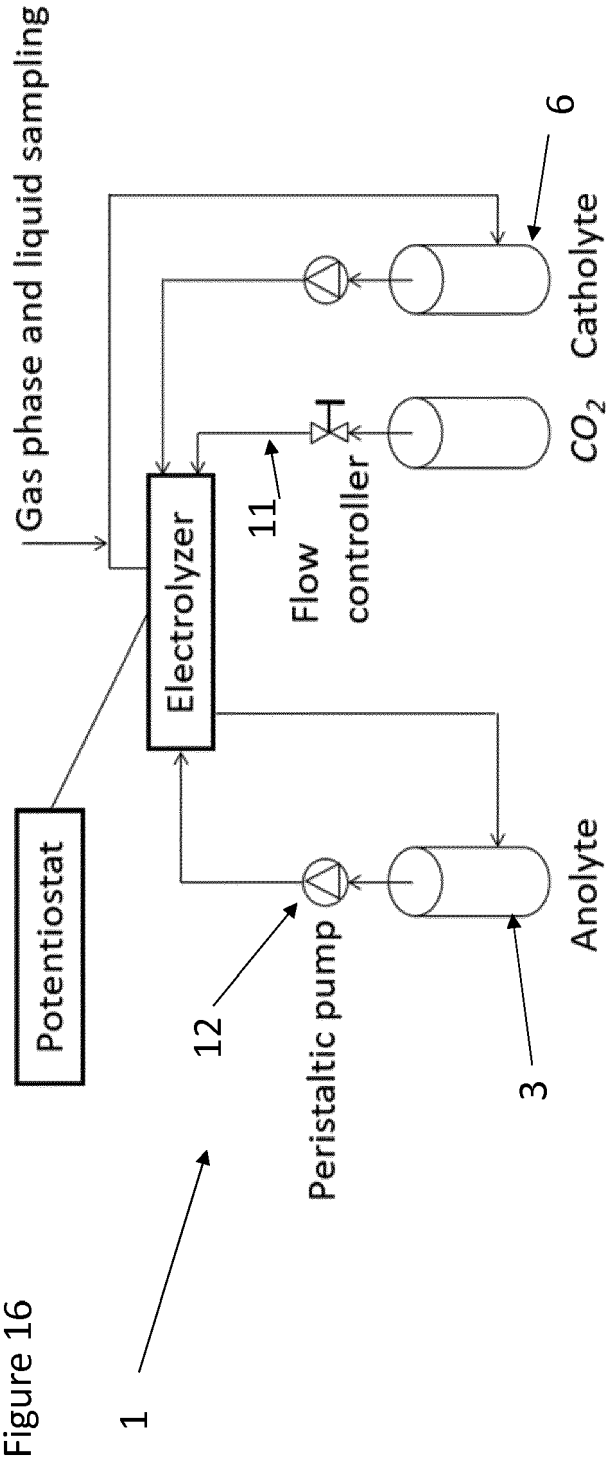
Gas phase and liquid sampling
6
Catholyte
CO_2
11
Flow controller
Electrolyzer
Potentiostat
12
Peristaltic pump
Analyte
3
1

Figure 16

Figure 17

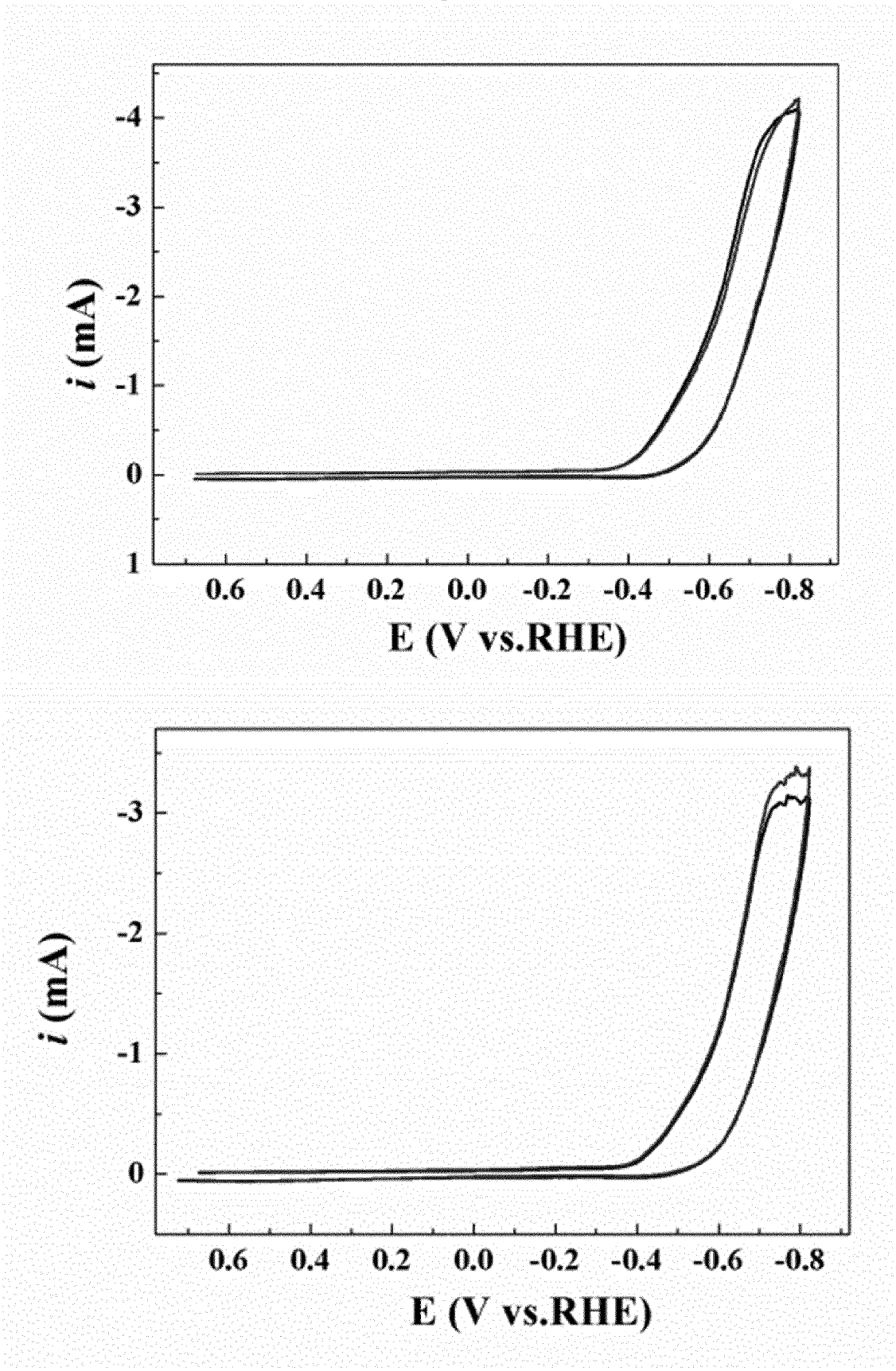
-4
-3
-2
-1
0
1
i (mA)
0.6
0.4
0.2
0.0
-0.2
-0.4
-0.6
-0.8
E (V vs.RHE)
-3
-2
-1
0
i (mA)
0.6
0.4
0.2
0.0
-0.2
-0.4
-0.6
-0.8
E (V vs.RHE)

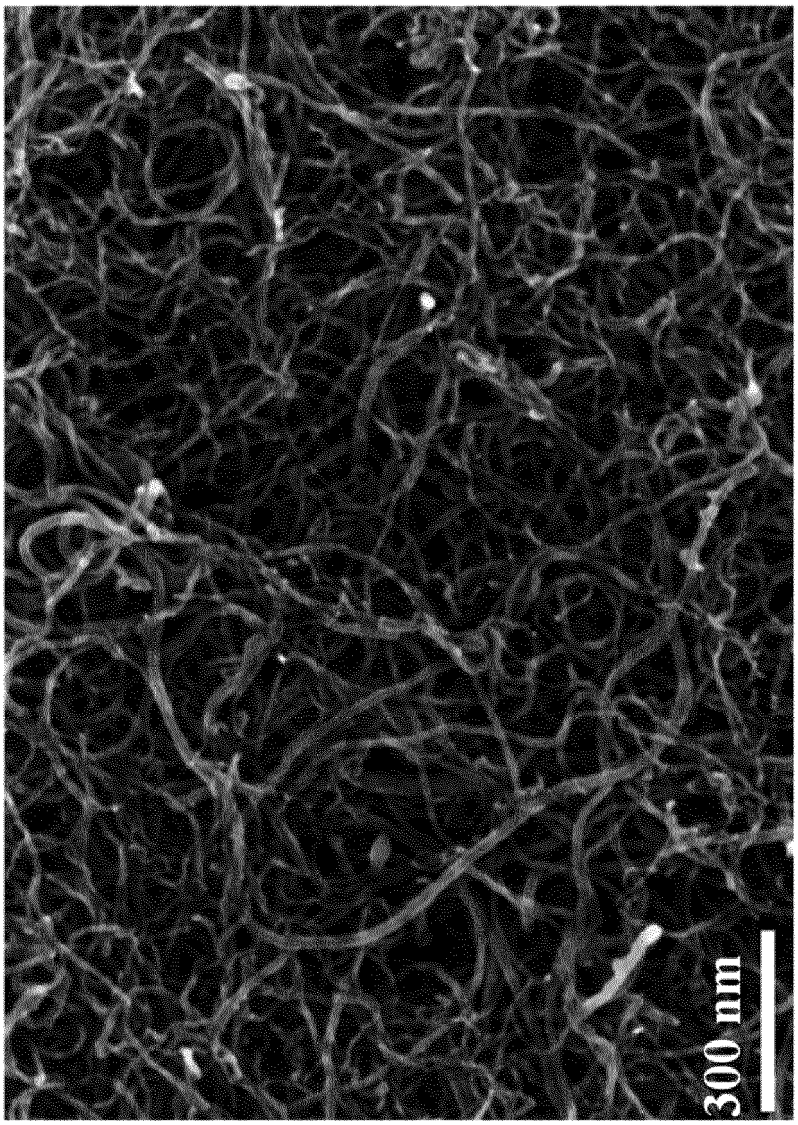

Figure 18

Figure 19

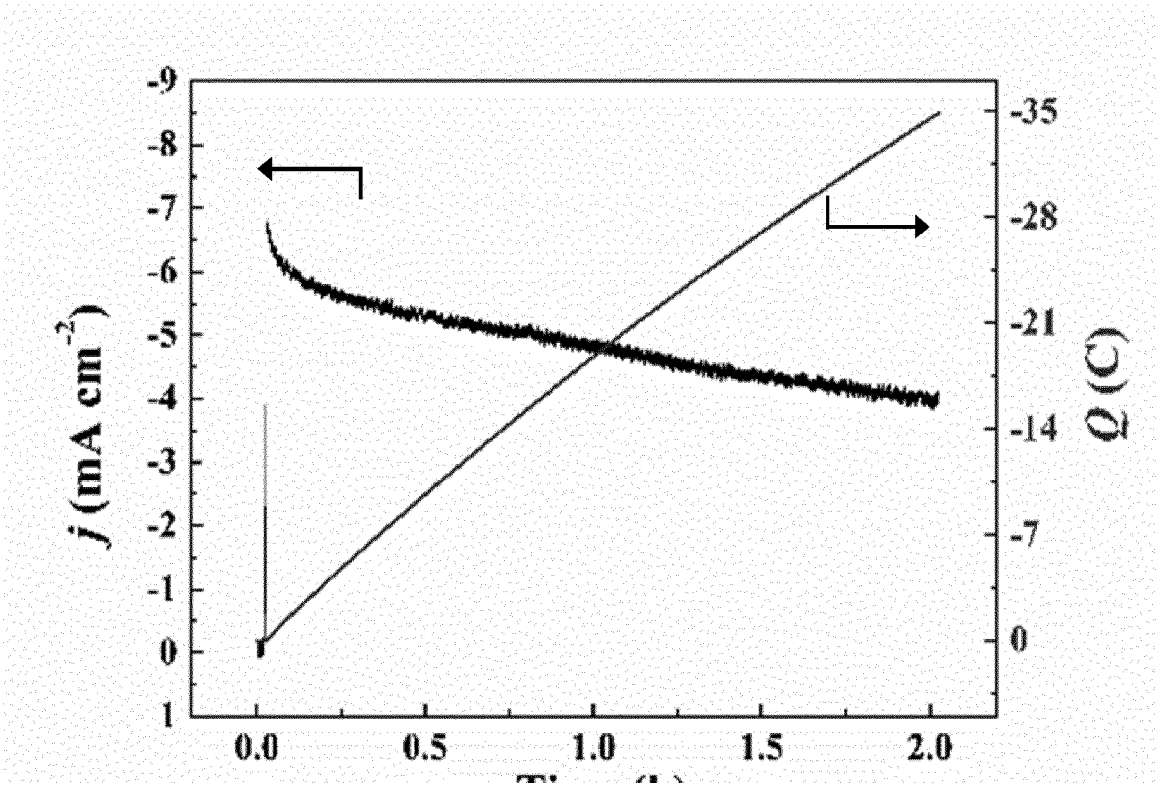
-9
-8
-7
-6
-5
-4
-3
-2
-1
0
1
j (mA cm-2)
-35
-28
-21
-14
-7
0
Q (C)
0.0
0.5
1.0
1.5
2.0

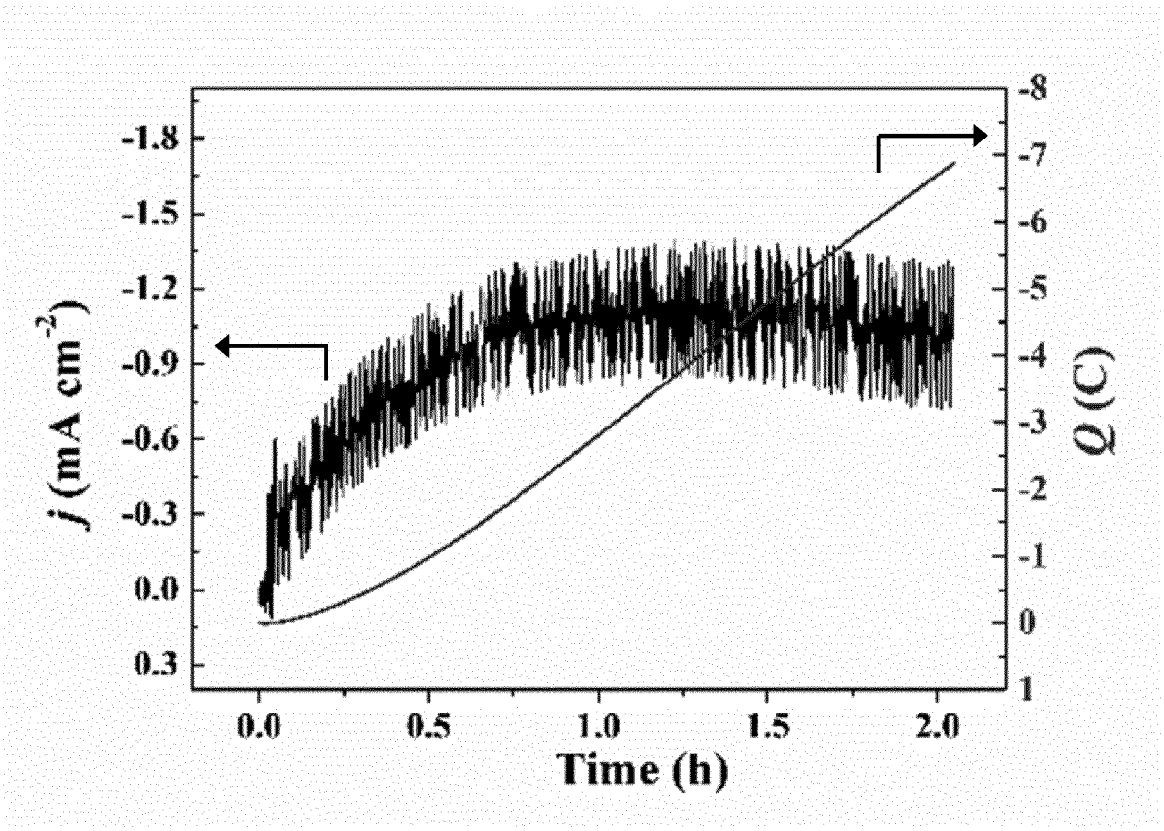
-1.8
-1.5
-1.2
-0.9
-0.6
-0.3
0.0
0.3
j (mA cm-2)
-8
-7
-6
-5
-4
-3
-2
-1
0
1
Q (C)
0.0
0.5
1.0
1.5
2.0
Time (h)

Figure 20

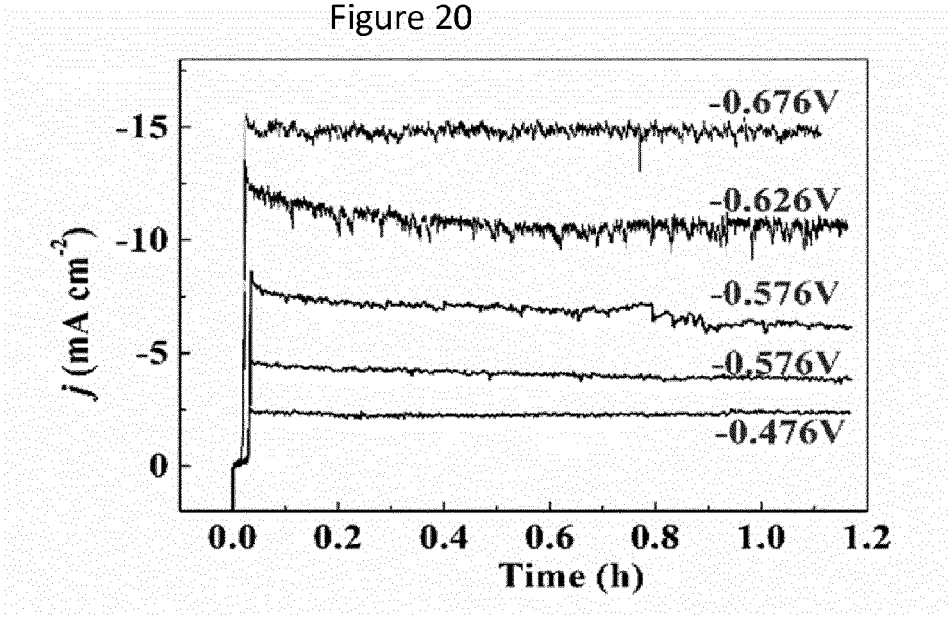

Figure 21

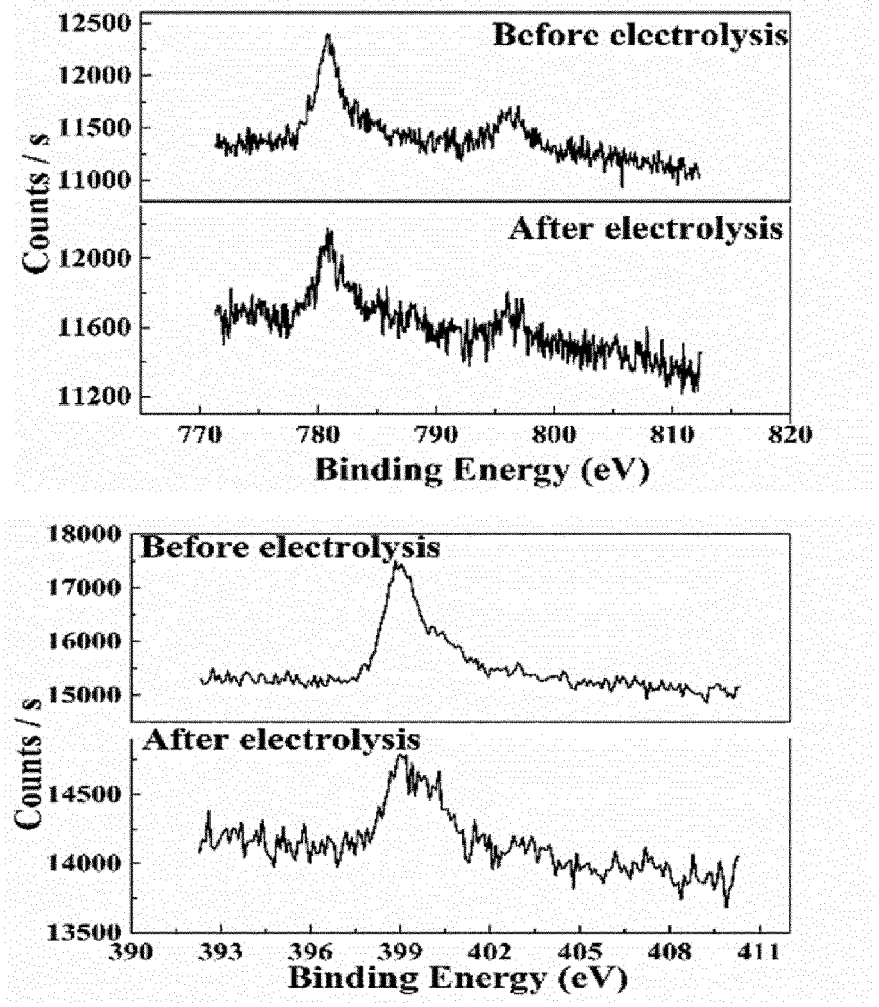

Figure 22

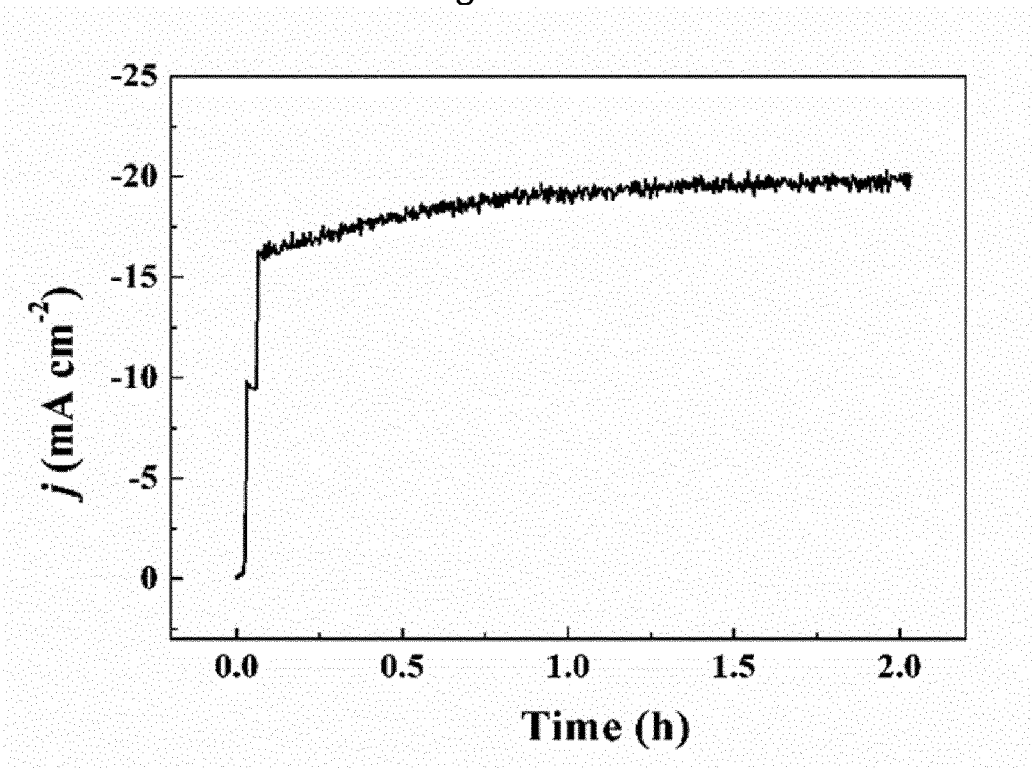

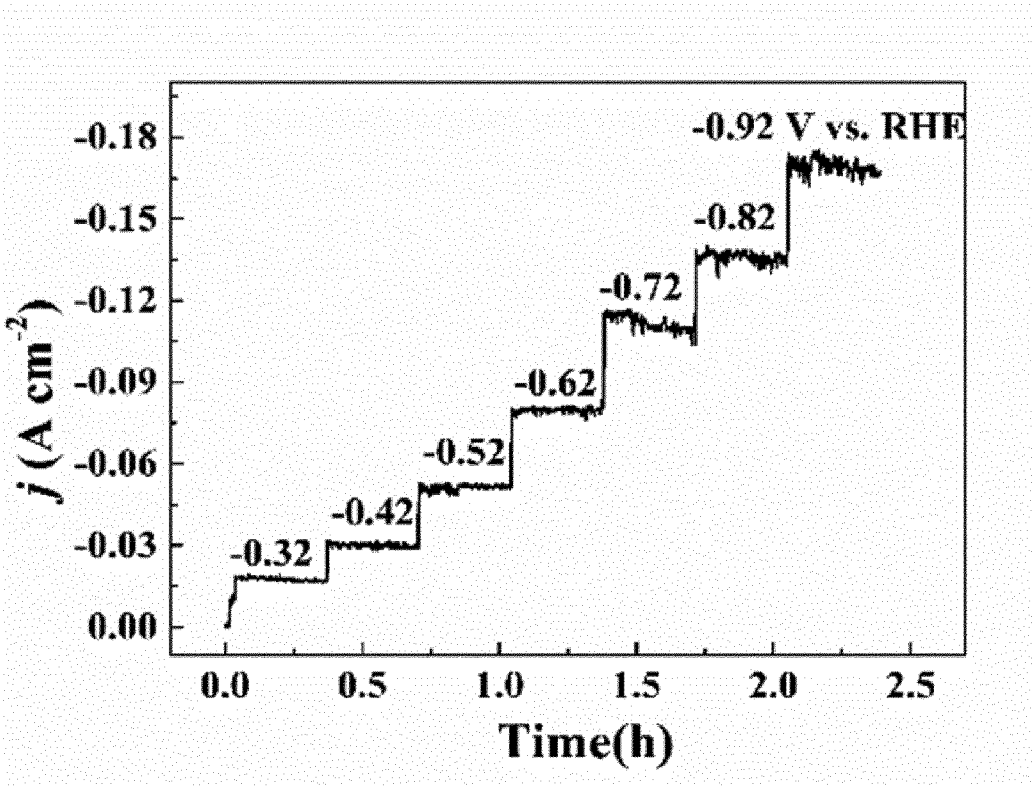

Figure 23

Figure 24

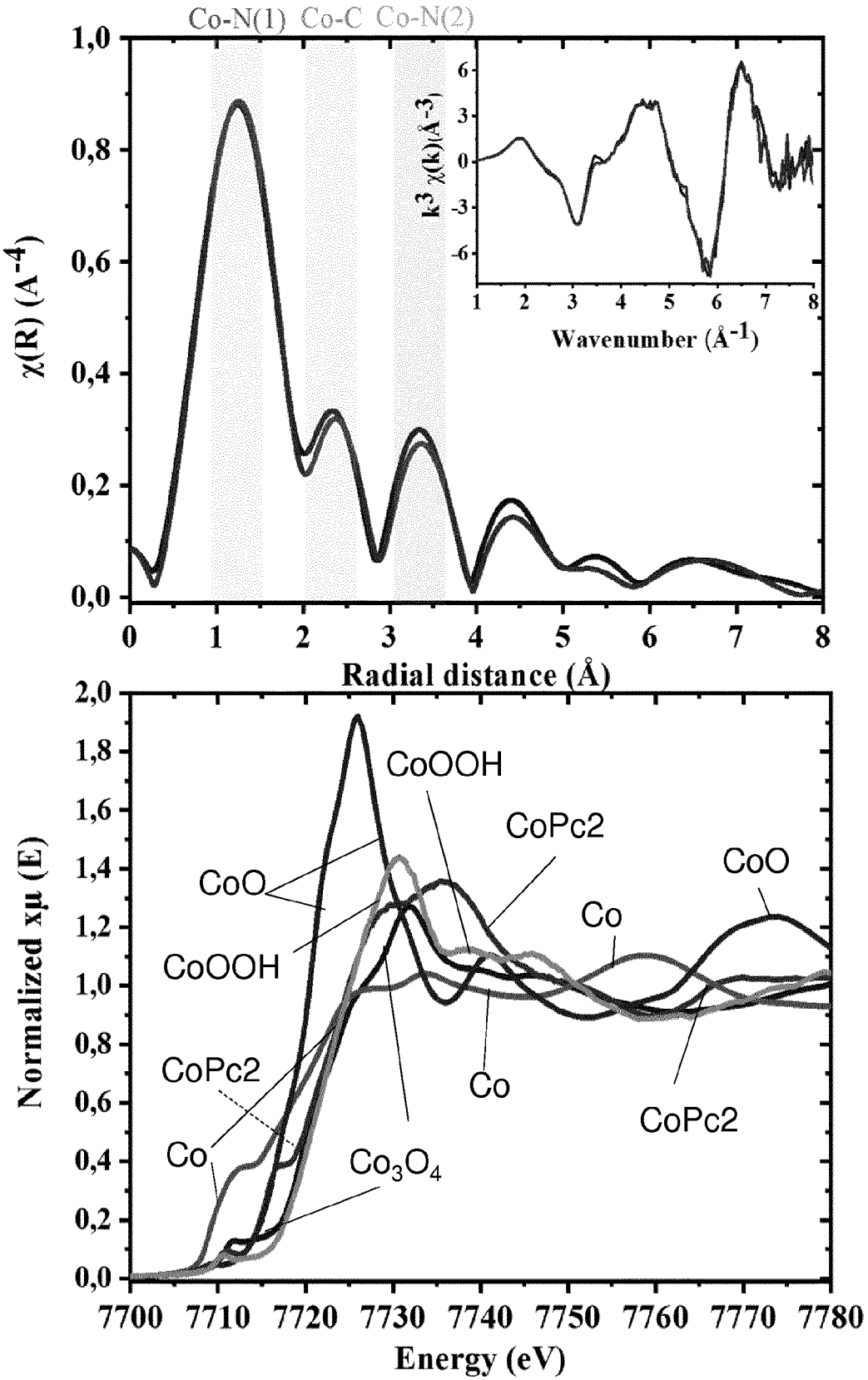
Co-N(1)
Co-C
Co-N(2)
χ(R) (A-4)
Radial distance (Å)
k3 χ(k)(Å-3)
Wavenumber (Å-1)
Normalized xμ (E)
Energy (eV)
CoO
CoOOH
CoPc2
Co
Co3O4

Figure 25

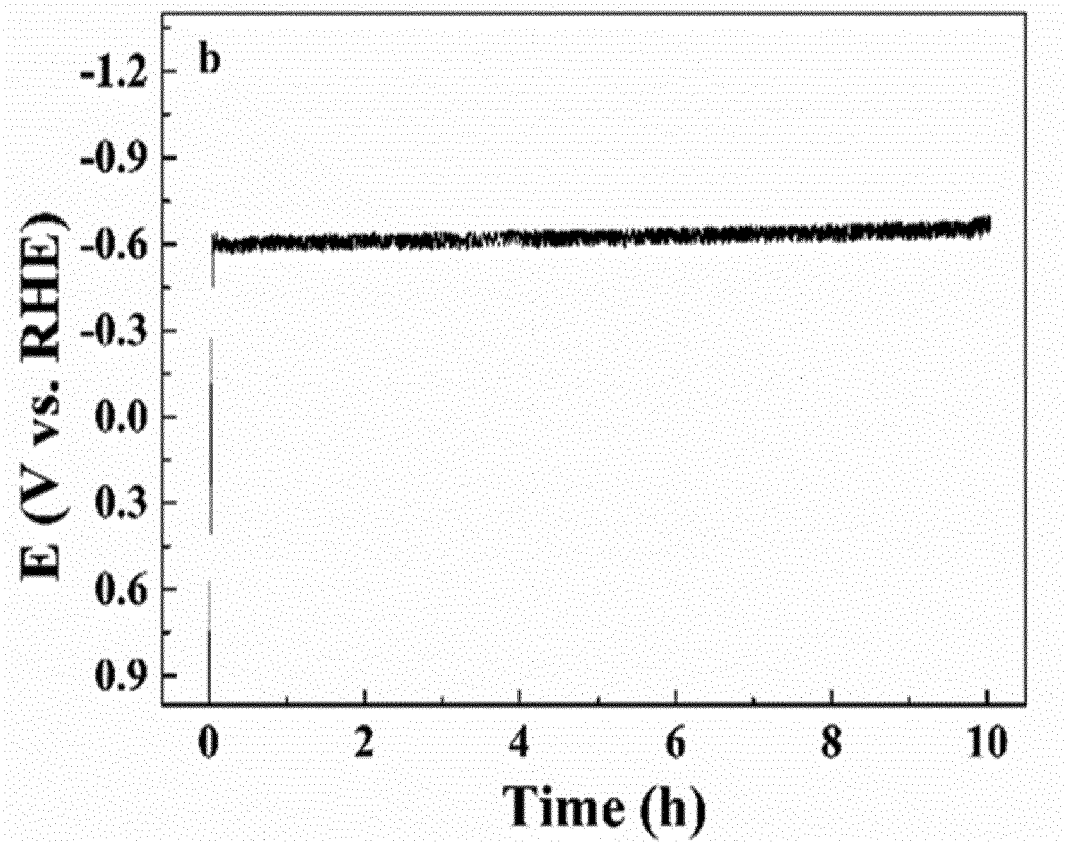

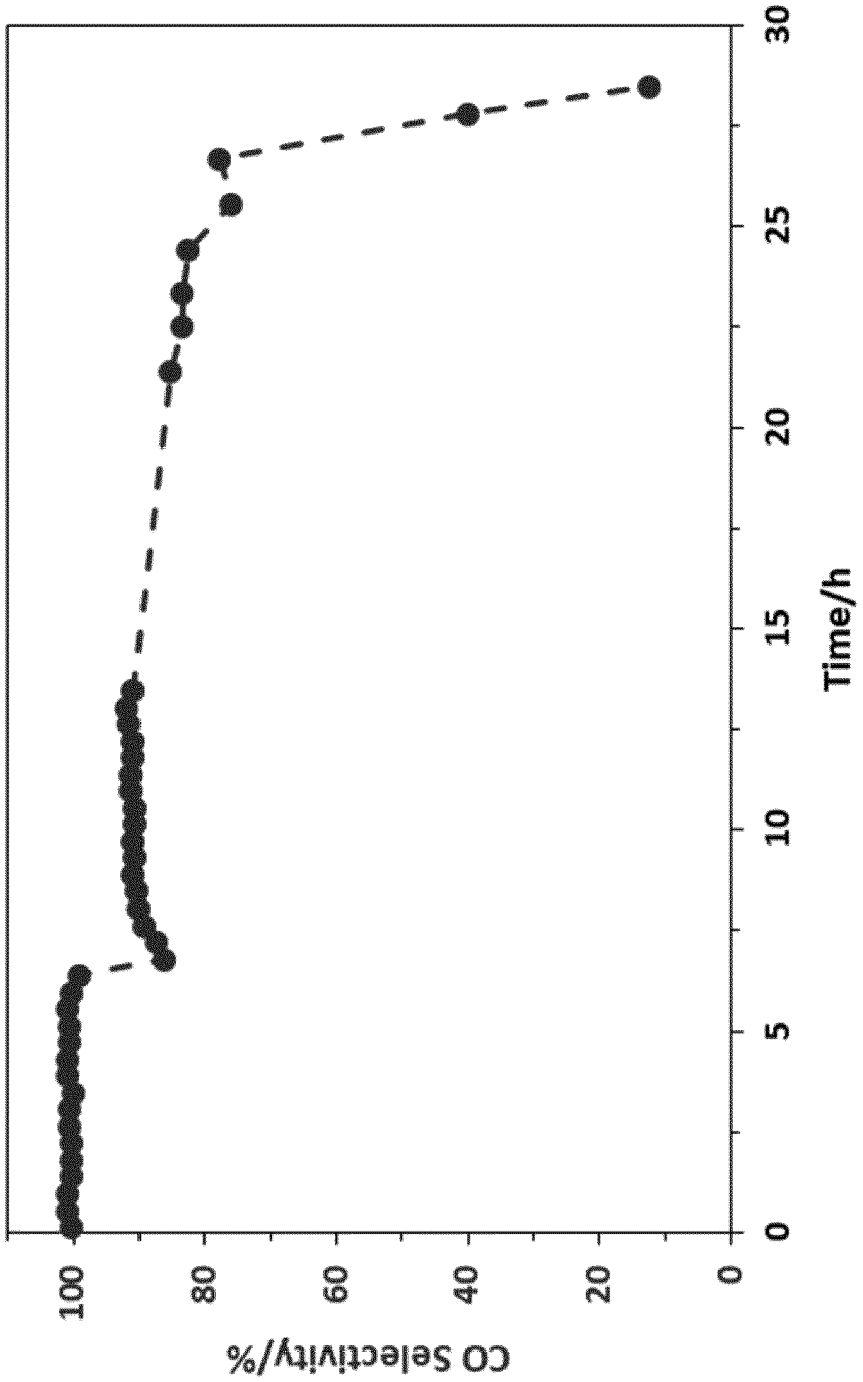

Figure 26

Europäisches Patentamt
European Patent Office
Office européen des brevets

EUROPEAN SEARCH REPORT

Application Number
EP 19 30 5971

DOCUMENTS CONSIDERED TO BE RELEVANT

Category	Citation of document with indication, where appropriate, of relevant passages	Relevant to claim	CLASSIFICATION OF THE APPLICATION (IPC)
Y	US 2018/066370 A1 (YAMADA ARISA [JP] ET AL) 8 March 2018 (2018-03-08) * the whole document * -----	1-18	INV. C25B1/00 C25B1/10 C25B9/08
Y	US 2018/023204 A1 (COSTENTIN CYRILLE [FR] ET AL) 25 January 2018 (2018-01-25) * the whole document * -----	1,2,4-6, 11-18	C25B11/04
Y	Tsukasa Yoshida ET AL: "Selective electrocatalysis for CO 2 reduction in the aqueous phase using cobalt phthalocyanine/poly-4-vinylpyridine modified electrodes", ELSEVIER Journal of Electroanalytical Chemistry, 1 January 1995 (1995-01-01), pages 209-225, XP055629133, Retrieved from the Internet: URL:https://www.sciencedirect.com/science/article/pii/002207289403762R/pdf?md5=44904d29621e1170fa3021cee5e99ab8&pid=1-s2.0-002207289403762R-main.pdf * the whole document * -----	1-3, 7-15,17, 18	TECHNICAL FIELDS SEARCHED (IPC) C25B
Y	MIN WANG ET AL: "A Hybrid Co Quaterpyridine Complex/Carbon Nanotube Catalytic Material for CO 2 Reduction in Water", ANGEWANDTE CHEMIE, INTERNATIONAL EDITION, vol. 57, no. 26, 22 May 2018 (2018-05-22), pages 7769-7773, XP055653460, DE ISSN: 1433-7851, DOI: 10.1002/anie.201802792 * the whole document * -----	1,2, 12-18	

The present search report has been drawn up for all claims

Place of search	Date of completion of the search	Examiner
Munich	21 January 2020	Ritter, Thomas

CATEGORY OF CITED DOCUMENTS

X : particularly relevant if taken alone
Y : particularly relevant if combined with another document of the same category
A : technological background
O : non-written disclosure
P : intermediate document

T : theory or principle underlying the invention
E : earlier patent document, but published on, or after the filing date
D : document cited in the application
L : document cited for other reasons

& : member of the same patent family, corresponding document

EPO FORM 1503 03.82 (P04C01)

ANNEX TO THE EUROPEAN SEARCH REPORT ON EUROPEAN PATENT APPLICATION NO. EP 19 30 5971

This annex lists the patent family members relating to the patent documents cited in the above-mentioned European search report. The members are as contained in the European Patent Office EDP file on
The European Patent Office is in no way liable for these particulars which are merely given for the purpose of information.

21-01-2020

Patent document cited in search report	Publication date	Patent family member(s)	Publication date
US 2018066370 A1	08-03-2018	JP 2018034136 A	08-03-2018
		US 2018066370 A1	08-03-2018
US 2018023204 A1	25-01-2018	CN 107636202 A	26-01-2018
		EP 3253905 A1	13-12-2017
		JP 2018512498 A	17-05-2018
		US 2018023204 A1	25-01-2018
		WO 2016124611 A1	11-08-2016

EPO FORM P0459

For more details about this annex : see Official Journal of the European Patent Office, No. 12/82

REFERENCES CITED IN THE DESCRIPTION

This list of references cited by the applicant is for the reader's convenience only. It does not form part of the European patent document. Even though great care has been taken in compiling the references, errors or omissions cannot be excluded and the EPO disclaims all liability in this regard.

Non-patent literature cited in the description

- *CHEMICAL ABSTRACTS,* 7782-42-5 **[0060]**
- **AZCARATE, I. ; COSTENTIN, C. ; ROBERT, M. ; SAVÉANT, J.-M.** Through-space charge interaction substituent effects in molecular catalysis leading to the design of the most efficient catalyst of CO2-to-CO electrochemical conversion. *J. Am. Chem. Soc.,* 2016, vol. 138, 16639-16644 **[0080]**
- **FRANCKE, R. ; SCHILLE, B. ; ROEMELT, M.** Homogeneously catalyzed electroreduction of carbon dioxide-Methods, mechanisms, and catalysts. *Chem. Rev.,* 2018, vol. 116, 4631-4701 **[0080]**
- **COSTENTIN, C. ; ROBERT, M. ; SAVÉANT, J.-M.** Catalysis of the electrochemical reduction of carbon dioxide. *Chem. Soc. Rev.,* 2013, vol. 42, 2423-2436 **[0080]**
- **QIAO, J. ; LIU, Y. ; HONG, F. ; ZHANG, J.** A review of catalysts for the electroreduction of carbon dioxide to produce low-carbon fuels. *Chem. Soc. Rev.,* 2014, vol. 43, 631-675 **[0080]**
- **ELGRISHI, N. ; CHAMBERS, M. B. ; WANG, X. ; FONTECAVE, M.** Molecular polypyridine-based metal complexes as catalysts for the reduction of CO. *Chem. Soc. Rev.,* 2017, vol. 46, 761-796 **[0080]**
- **GRICE, K. A.** Carbon dioxide reduction with homogenous early transition metal complexes: Opportunities and challenges for developing CO2 catalysis. *Coord. Chem. Rev. 336,* 2017, 78-95 **[0080]**
- **GRILLS, D. C. ; ERTEM, M. Z ; MCKINNON, M. ; NGO, K. T. ; ROCHFORD, J.** Mechanistic aspects of CO2 reduction catalysis with manganese-based molecular catalysts. *Coord. Chem. Rev.,* 2018, vol. 374, 173-217 **[0080]**
- **LOEWEN, N. D. ; NEELAKANTAN, T. V. ; BERBEN, L. A.** Renewable formate from C-H bond formation with CO2: using iron carbonyl clusters as electrocatalysts. *Acc. Chem. Res.,* 2017, vol. 50, 2362-2370 **[0080]**
- **TAKEDA, H. ; COMETTO, C. ; ISHITANI, O. ; ROBERT, M.** Electrons, photons, protons and earth abundant metal complexes for molecular catalysis of CO2 reduction. *ACS Catal.,* 2017, vol. 7, 70-88 **[0080]**
- **WANG, M. ; CHEN, L. ; LAU, T-C. ; ROBERT, M.** Hybrid Co quaterpyridine complex /carbon nanotube catalytic material for CO2 reduction in water. *Angew. Chem. Int. Ed.,* 2018, vol. 57, 7769-7773 **[0080]**
- **XU, L. ; WU, Y. ; YUAN, X. ; HUANG, L. ; WU, Z. ; XUAN, J. ; WANG, Y. ; WANG. H.** High-Performance Electrochemical CO2 Reduction Cells Based on Non-noble Metal Catalysts. *ACS Energy Lett.,* 2018, vol. 3, 2527-2532 **[0080]**
- **KUTZ, R. B. ; CHEN, Q. ; YANG, H. ; SAJJAD, S. D. ; LIU, Z. ; MASEL, I. R.** Sustainion imidazolium-functionalized polymers for carbon dioxide electrolysis. *Energy Technol.,* 2017, vol. 5, 929-936 **[0080]**
- **DINH, C-T. ; GARCIA DE ARQUER, F. P. ; SINTON, D. ; SARGENT, E. H.** High Rate, Selective, and Stable Electroreduction of CO2 to CO in Basic and Neutral Media. *ACS Energy Lett.,* 2018, vol. 3, 2835-2840 **[0080]**
- **VERMA, S. ; HAMASAKI, Y. ; KIM, C. ; HUANG, W. ; LU, S. ; JHONG, H-R. M. ; GEWIRTH, A. A. ; FUJIGAYA, T. ; NAKASHIMA, N. ; KENIS, P. J. A.** Insights into the low overpotential electroreduction of CO2 to CO on a supported gold catalyst in an alkaline flow electrolyzer. *ACS Energy Lett.,* 2018, vol. 3, 193-198 **[0080]**
- **ZHANG, X. ; WU, Z ; ZHANG, X. ; LI, L. ; LI, Y. ; XU, H. ; LI, X. ; YU, X. ; ZHANG, Z. ; LIANG, Y.** Highly selective and active CO2 reduction electrocatalysts based on cobalt phthalocyanine/carbon nanotube hybrid structures. *Nat. Commun.,* 2017, vol. 8, 14675 **[0080]**
- **HAN, N. ; WANG, Y. ; MA, L. et al.** Supported cobalt phthalocyanine for high-performance electrocatalytic CO2 reduction. *Chem,* 2017, vol. 3, 652-664 **[0080]**
- **LI, N. ; LU, W. ; PEI K. ; CHEN, W.** *Interfacial peroxidase-like catalytic activity of surface-immobilized cobalt phthalocyanine on multiwall carbon nanotubes RSC Advances,* 2015, vol. 5, 9374-9380 **[0080]**
- **WANG M. ; CHEN L. G. ; LAU T.-C. ; ROBERT M. A.** Hybrid Co Quaterpyridine Complex/Carbon Nanotube Catalytic Material for CO2 Reduction in Water. *Angew. Chem.,* 2018, vol. 130, 7895-7899 **[0080]**